chains induce pH-selective, endosomal membrane destabilization with amplified transfection and negligible cytotoxicity, J. Am. Chem. Soc. 130 (2008) 16287–16294.
[8] N. Kanayama, S. Fukushima, N. Nishiyama, K. Itaka, W.-D. Jang, K. Miyata, Y. Yamasaki, U.-I. Chung, K. Kataoka, A PEG-based biocompatible block catiomer with high buffering capacity for the construction of polyplex micelles showing efficient gene transfer toward primary cells, ChemMedChem 1 (2006) 439–444.
[9] K. Masago, K. Itaka, N. Nishiyama, U.-I. Chung, K. Kataoka, Gene delivery with biocompatible cationic polymer: pharmacogenomic analysis on cell bioactivity, Biomaterials 28 (2007) 5169–5179.
[10] D. Akagi, M. Oba, H. Koyama, N. Nishiyama, S. Fukushima, T. Miyata, H. Nagawa, K. Kayaoka, Biocompatible micellar nanovectors achieve efficient gene transfer to vascular lesions without cytotoxicity and thrombus formation, Gene Ther. 14 (2007) 1029–1038.
[11] M. Harada-Shiba, I. Takamisawa, K. Miyata, T. Ishii, N. Nishiyama, K. Itaka, K. Kangawa, F. Yoshihara, Y. Asada, K. Hatakeyama, N. Nagaya, K. Kataoka, Intratracheal gene transfer of adrenomedullin using polyplex nanomicelles attenuates monocrotaline-induced pulmonary hypertension in rats, Mol. Ther. 17 (2009) 1180–1186.
[12] K. Miyata, M. Oba, M.R. Kano, S. Fukushima, Y. Vachutinsky, M. Han, H. Koyama, K. Miyazono, N. Nishiyama, K. Kataoka, Polyplex micelles from triblock copolymers composed of tandemly aligned segments with biocompatible, endosomal escaping, and DNA-condensing functions for systemic gene delivery to pancreatic tumor tissue, Pharm. Res. 25 (2008) 2924–2936.
[13] K. Itaka, S. Ohba, K. Miyata, H. Kawaguchi, K. Nakamura, T. Takato, U.-I. Chung, K. Kataoka, Bone regeneration by regulated in vivo gene transfer using biocompatible polyplex nanomicelles, Mol. Ther. 15 (2007) 1655–1662.
[14] S.C. de Smedt, J. Demeester, W.E. Hennink, Cationic polymer based gene delivery systems, Pharm. Res. 17 (2000) 113–126.
[15] Y. Wang, S. Gao, W.-H. Ye, H.S. Yoon, Y.-Y. Yang, Co-delivery of drugs and DNA from cationic core-shell nanoparticles self-assembled from a biodegradable copolymer, Nat. Mater. 5 (2006) 791–796.
[16] A. Alshamsan, A. Haddadi, V. Incani, J. Samuel, A. Lavasanifar, H. Uludag, Formulation and delivery of siRNA by oleic acid and stearic acid modified polyethylenimine, Mol. Pharm. 6 (2009) 121–133.
[17] W.J. Kim, L.V. Christensen, S. Jo, J.W. Yockman, J.H. Jeong, Y. -H. Kim, S. W. Kim, Cholesteryl oligoarginine delivering vascular endothelial growth factor siRNA effectively inhibits tumor growth in colon adenocarcinoma, Mol. Ther. 14 (2006) 343–350.
[18] A. Harada, K. Kataoka, Formation of polyion complex micelles in an aqueous milieu from a pair of oppositely-charged block copolymers with poly(ethylene glycol) segments, Macromol. 28 (1995) 5294–5299.
[19] M. Ocker, D. Neureiter, M. Lueders, S. Zopf, M. Ganslmayer, E.G. Hahn, C. Herold, D. Schuppan, Variants of bcl-2 specific siRNA for silencing antiapoptotic bcl-2 in pancreatic cancer, Gut 54 (2005) 1298–1308.
[20] K. de Bruin, N. Ruthardt, K. von Gersdorff, R. Bausinger, E. Wagner, M. Ogris, C. Bräuchle, Cellular dynamics of EGF receptor-targeted synthetic viruses, Mol. Ther. 15 (2007) 1297–1305.
[21] A.P. French, S. Mills, R. Swarup, M.J. Bennett, T.P. Pridmore, Colocalization of fluorescent markers in confocal microscope images of plant cells, Nat. Protoc. 3 (2008) 619–628.
[22] M. Meyer, A. Philipp, R. Oskuee, C. Schmidt, E. Wagner, Breathing life into polycations: functionalization with pH-responsive endosomolytic peptides and polyethylene glycol enables siRNA delivery, J. Am. Chem. Soc. 130 (2008) 3272–3273.
[23] J. DeRouchey, C. Schmidt, G.F. Walker, C. Koch, C. Plank, E. Wagner, J.O. Rädler, Monomolecular assembly of siRNA and poly(ethylene glycol)-peptide copolymers, Biomacromolecules 9 (2008) 724–732.
[24] L.M. Ellis, D.J. Hicklin, VEGF-targeted therapy: mechanisms of anti-tumour activity, Nat. Rev. Cancer 8 (2008) 579–591.
[25] D.S. Ziegler, A.L. Kung, Therapeutic targeting of apoptosis pathways in cancer, Curr. Opin. Oncol. 20 (2008) 97–103.
[26] J. George, N.L. Banik, S.K. Ray, Bcl-2 siRNA augments taxol mediated apoptotic death in human glioblastoma U138MG and U251MG cells, Neurochem. Res. 34 (2009) 66–78.

Biomaterials 31 (2010) 3707–3714

Contents lists available at ScienceDirect

Biomaterials

journal homepage: www.elsevier.com/locate/biomaterials

Biodegradable polyamino acid-based polycations as safe and effective gene carrier minimizing cumulative toxicity

Keiji Itaka [a,d,1], Takehiko Ishii [b,d,1], Yoko Hasegawa [a,d], Kazunori Kataoka [a,b,c,d,*]

[a] Division of Clinical Biotechnology, Center for Disease Biology and Integrative Medicine, Graduate School of Medicine, The University of Tokyo, 7-3-1 Hongo, Bunkyo-ku, Tokyo 113-0033, Japan
[b] Department of Bioengineering, Graduate School of Engineering, The University of Tokyo, 7-3-1 Hongo, Bunkyo-ku, Tokyo 113-0033, Japan
[c] Department of Materials Science and Engineering, Graduate School of Engineering, The University of Tokyo, 7-3-1 Hongo, Bunkyo-ku, Tokyo 113-0033, Japan
[d] Center for NanoBio Integration, The University of Tokyo, 7-3-1 Hongo, Bunkyo-ku, Tokyo 113-0033, Japan

ARTICLE INFO

Article history:
Received 4 November 2009
Accepted 23 November 2009
Available online 13 February 2010

Keywords:
Non-viral gene carrier
Cationic polymer
Biodegradable polycation
Polyplex
Cumulative toxicity

ABSTRACT

Gene delivery using cationic polymers has attracted much attention due to their potential advantages, such as large DNA loading capacity, ease of large-scale production, and reduced immunogenicity. We recently reported that polyplexes from poly[N-[N-(2-aminoethyl)-2-aminoethyl]aspartamide] (P[Asp(DET)]), having an efficient endosomal escape due to pH-selective membrane destabilization, showed high transfection efficiency with minimal toxicity. Pharmacogenomic analysis demonstrated that P[Asp(DET)] also provided long-term security after transfection. We hypothesized that the biodegradability of P[Asp(DET)] played a significant role in achieving effective transfection. Gel permeation chromatography (GPC) and electrospray ionization mass spectrometry (ESI-MS) measurements of P[Asp(DET)] revealed their ability to undergo rapid degradation. In contrast, a derivative polycation, N-substituted polyglutamide (P[Glu(DET)]), showed no degradability, indicating that the degradation of P[Asp(DET)] was induced by a specific self-catalytic reaction between the PAsp backbone and the side-chain amide nitrogen. Degradation products of P[Asp(DET)] caused no cytotoxicity, even at high concentrations in the culture medium. Repeated transfection by administering the polyplexes for every 24 h showed that biodegradable P[Asp(DET)] provided a continuous increase in transgene expression, while non-degradable P[Glu(DET)] showed a decrease in transgene expression after 48 h, coupled with fluctuations in expression profiles of endogenous genes. *In vivo* intraperitoneal injection of P[Asp(DET)] induced minimal inflammatory cytokine induction to a level comparable to that of normal saline. These results indicate that the biodegradability of P[Asp(DET)] played a key role in achieving safe and sustained transgene expression, by minimizing cumulative toxicity caused by polycations remaining in cells or in the body.

1. Introduction

Applications of gene therapy have been considered in many clinical fields. Safe and efficient gene introduction are prerequisites for successful gene therapy. During the past decade, various cationic polymers have attracted much attention for use as non-viral gene carriers, as they have many potential advantages, such as large DNA loading capacity, ease of large-scale production, and reduced immunogenicity that has been an issue associated with the use of viral vectors [1–3].

Among these polymers, polyethylenimine (PEI) and its derivatives have been extensively investigated due to their excellent transfection efficiencies [4]. However, their clinical use has been limited primarily due to their toxicities. We recently found a flanking benzyl ester group of poly(β-benzyl L-aspartate) (PBLA) that underwent a quantitative aminolysis reaction with a variety of amine compounds under very mild condition. Using this reaction, we prepared an N-substituted poly(aspartamide) (PAsp) derivative library possessing a variety of cationic side chains from a single PBLA platform. Through a series of transfection and cytotoxicity assays using this library, a highly promising candidate, poly[N-[N-(2-aminoethyl)-2-aminoethyl]aspartamide] (P[Asp(DET)]) was emerged to show high capacity with minimal toxicity (Fig. 1) [5].

* Corresponding author at: Department of Materials Engineering, Graduate School of Engineering, The University of Tokyo, 7-3-1 Hongo, Bunkyo-ku, Tokyo 113-0033, Japan. Tel.: +81 3 5841 7138; fax: +81 3 5841 7139.
E-mail address: kataoka@bmw.t.u-tokyo.ac.jp (K. Kataoka).

[1] The first two authors contributed equally to this work.

0142-9612/$ – see front matter © 2009 Elsevier Ltd. All rights reserved.
doi:10.1016/j.biomaterials.2009.11.072

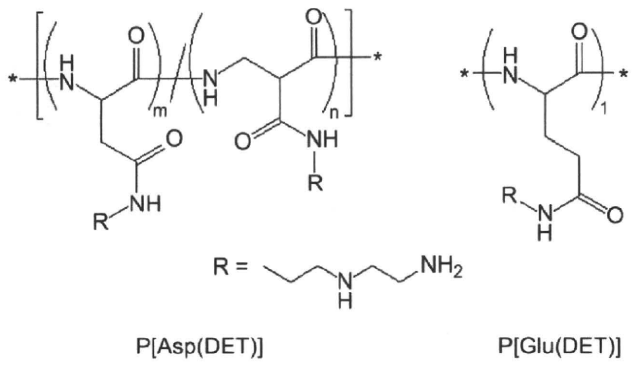

Fig. 1. Molecular structures of P[Asp(DET)] and P[Glu(DET)].

P[Asp(DET)] showed an excellent transgene expression comparable to a commercially available linear PEI (ExGen 500) and a lipid-based system (LipofectAMINE 2000) [6]. By the form of PEGylated polyplexes (polyplex micelle; poly(ethylene glycol) (PEG)-P[Asp(DET)] block copolymer/pDNA), we have successfully introduced the transgene into aminal models, such as (i) a rabbit's clamped carotid artery with neointima via intra-arterial injection15 [7], (ii) a mouse skull by regulated release from a calcium phosphate cement scaffold to induce bone regeneration through differentiation factor transduction [8], and (iii) a mouse lung via intratracheal administration to cure pulmonary hypertension by introducing the adrenomedullin gene [9].

Safe and efficient gene introduction using (PEG-)P[Asp(DET)] has been attributed to its unique 1,2-diaminoethane side chain, where the N-(2-aminoethyl)-2-aminoethyl group exhibits a distinctive two-step protonation behavior [5]. This dual protonation state suggests that strong pH-buffering capacity of P[Asp(DET)] units was responsible for an efficient endosomal escape, which has often been explained as the mechanism underlying the excellent transfection efficiency of PEI. In addition, we recently found that pH-selective membrane destabilization by P[Asp(DET)] played a key role in an efficient endosomal escape of P[Asp(DET)]/DNA polyplexes into the cytoplasm [10]. The reduced cytotoxicity caused by P[Asp(DET)] was attributed with its limited interactions with other plasma and cytoplasmic membranes at neutral pH.

Another important aspect in achieving a good therapeutic effect is the long-term security of the polymers. We have already shown that, when used in application with primary cells, P[Asp(DET)] induces cell differentiation more effectively than that by other commercially available reagents [8]. Pharmacogenomic analysis suggested that P[Asp(DET)] maintained cellular homeostasis after transfection [6]. Although comparable reporter gene expression and cell viability were obtained after a few days of transfection, the efficacy of inducing cell differentiation differed significantly among the reagents. The carrier materials complexed with DNA inevitably remain within cells after releasing the DNA, either in the cytoplasm or nucleus. Thus, it is reasonable to assume that the safety of the polymers remaining within cells may significantly affect cell behavior.

For this study, we hypothesized that this aspect of safety would be strongly attributed to the biodegradability of P[Asp(DET)]. We compared the physicochemical properties underlying the degradability of P[Asp(DET)] with that of a non-degradable derivative polymer. Sustained transgene expression and cell viability were demonstrated with *in vitro* assays using cultured cells. Finally, cytokine induction after *in vivo* administration of polymers was determined to evaluate the feasibility of therapeutic uses of these polymers.

2. Materials and methods

2.1. Materials

β-benzyl-L-aspartate N-carboxy-anhydride (BLA-NCA) was synthesized according to Fuchs' method. N-Methyl-2-pyrrolidone (NMP) was purchased from Nacalai tesque Inc. (Kyoto, Japan). *n*-Buthylamine, benzene, N,N-dimethylformamide (DMF) and dichloromethane (CH_2Cl_2) were purchased from Wako Pure Chemical Industries, Ltd. (Osaka, Japan). 2-Hydroxypyridine was purchased from Aldrich Chem. Co. (Milwaukee, WI, USA), distilled under reduced pressure, and recrystalized from ethanol. Diethylenetriamine (DET) was purchased from Tokyo Chemical Industry (Tokyo, Japan). For chemical reactions, *n*-buthylamine, DET, and NMP were distilled from calcium hydride (CaH_2) under reduced pressure. DMF and CH_2Cl_2 were purified by passing through two packed columns of neutral alumina (Glass Contour, Irvine, CA, USA).

Plasmid DNAs (pDNA) encoding firefly luciferase (pGL4.13: Promega, Madison, WI, USA) and renilla luciferase (pRL-CMV: Promega) were amplified in competent DH5α Escherichia coli and purified using NucleoBond Xtra EF (Nippon Genetics, Tokyo, Japan). The pDNA concentration was determined from the absorbance at 260 nm. Dulbecco's modified Eagle's medium (DMEM) and fetal bovine serum (FBS) were purchased from Sigma–Aldrich (St. Louis, MO, USA) and Life Technologies Japan Ltd. (Tokyo, Japan), respectively. Linear polyethylenimine (LPEI) (Exgen 500, MW = 22 kDa) was purchased from MBI Fermentas (Burlington, ON, Canada). Lipopolysaccharide (LPS: L4391) was purchased from Sigma–Aldrich.

2.2. Cells and animals

Human hepatoma cells (HuH-7) and human umbilical vein endothelial cells (HUVEC) were obtained from the Japanese Collection of Research Bioresources Cell Bank (Tokyo, Japan) and Lonza Ltd. (Basel, Switzerland), respectively. Bioluminescent cells (HuH-7-luc) stably expressing firefly luciferase were kindly provided by Mr. S. Matsumoto (The University of Tokyo).

Female ICR mice were purchased from Charles River Laboratories (Tokyo, Japan). All animal experimental protocols were performed in accordance with the guidelines of the Animal Committee of the University of Tokyo.

2.3. Preparation of poly(β-benzyl-L-aspartate) (PBLA) and poly(γ-benzyl-L-glutamate) (PBLG)

To obtain PBLA, BLA-NCA (1.2 g, 5 mmol) was dissolved in DMF (2 mL), diluted with CH_2Cl_2 (20 mL), and *n*-butylamine (10-fold dilution with CH_2Cl_2, 0.045 mL, 0.045 mmol) was added to initiate the ring-opening polymerization of NCA. The reaction solution was stirred for two days at 35 °C. All these procedures were performed under an argon atmosphere. PBLA was recovered by precipitation in an excess amount of *n*-hexane/AcOEt (6:4), and the filtrate was dried in vacuo. PBLG was prepared in a similar manner, except using BLG-NCA as a monomer. PBLA and PBLG obtained were analyzed at 40 °C using a gel permeation chromatography (GPC) system (TOHSO HLC-8220, Japan) equipped with TSK-gel Super AW4000 and Super AW3000 × 2 in series, as well as an internal refractive index (RI) detector, and confirmed to be unimodal with narrow distribution ($M_w/M_n = 1.06$ and 1.11, respectively). NMP containing 50 mM lithium bromide was used as an eluent. PEG standards were used to calibrate the molecular weight and the molecular weight distribution. From the ^{1}H nuclear magnetic resonance (NMR) spectra of PBLA and PBLG, their polymerization degrees were confirmed to be 102 and 89, respectively (d_6-DMSO at 80 °C, Supplemental Fig. S1).

2.4. Preparation of N-substituted polyaspartamide, P[Asp(DET)]

N-substituted polyaspartamides were prepared through the aminolysis reaction of PBLA. Lyophilized PBLA (50 mg) was dissolved in NMP (2 mL), and cooled to 0 °C. In another reaction tube, DET (50-fold excess molar to the benzyl ester units) was diluted twice with NMP, and cooled at 0 °C. The PBLA solution was added dropwise into the DET solution. After 1 h of reaction, the reaction mixture was added dropwise into a well-chilled 5 N HCl aqueous solution (equimolar amount to the added amino groups), where the temperature was kept below 10 °C. Then the mixture was first dialyzed against an aqueous solution of 0.01 N HCl and then against de-ionized water at 4 °C in a dialysis tube (MWCO: 6–8000). The final solution was lyophilized, and objective P[Asp(DET)] was obtained as the chloride salt form with a good yield. Quantitative introduction of DET was confirmed by ^{1}H NMR spectrum (Supplemental Fig. S2).

2.5. Preparation of N-substituted polyglutamide, P[Glu(DET)]

The ester-amide exchange reaction of PBLG was performed using DET in the presence of 2-hydroxypyridine as a catalyst according to the literature [11]. PBLG (0.2 g, 0.95 mmol) and 2-hydoxypyridine (452 mg, 5 eq.) were dissolved in DMF (4 mL), followed by the addition of DET (2 mL, 20-fold molar excess of benzyl ester units). After stirring the mixture for 30 h at 25 °C, it was treated in a similar manner with polyaspartamides as described above. Due to a small amount of undesirable

side reactions, such as cross-linking, additional purification was performed using a fractional preparative GPC system equipped with Superdex 200 pg XK50/60 column (GE healthcare, UK) and UV detector set at 220 nm. Phosphate buffer solution (10 mM, pH 7.4) containing 0.5 M NaCl was used as an eluent at a flow rate of 15 mL/min at room temperature. The main peak fractions were combined and dialyzed first against an aqueous solution of 0.01 N HCl, and then against de-ionized water at 4 °C. The final solution was lyophilized, and P[Glu(DET)] was obtained in the chloride salt form. Quantitative introduction of DET was confirmed by ^{1}H NMR spectrum (Supplemental Fig. S2).

2.6. Time-course GPC measurements

Time-course degradation profiles of P[Asp(DET)] and P[Glu(DET)] were evaluated using a GPC system (Jasco, Tokyo, Japan) equipped with Superdex 75 10/300 GL column (GE Healthcare UK, Ltd.) and UV detector set at 220 nm. Phosphate buffer solution (10 mM) containing 0.5 M NaCl was used as an eluent at a flow rate of 0.75 mL/min at room temperature. All samples were dissolved in citrate buffer (pH 3.0), acetate buffer (pH 5.5), phosphate buffer (pH 7.4), or carbonate buffer (pH 9.0) solution containing 0.15 M NaCl. These were stored at 4 °C, 25 °C, and 37 °C and analyzed at defined time points.

2.7. Electrospray ionization mass spectrometry (ESI-MS) measurements

P[Asp(DET)] (5 mg) was dissolved in Milli-Q water (5 mL) adjusting the pH to 7.4, sterilized by filtration (0.1 μm pore size), and incubated at 37 °C for one month. ESI-MS (AccuoTOF, JEOL, Tokyo, JAPAN) was conducted in the positive ion mode with an atmospheric pressure ionization electrospray interface, flushed with heated dry nitrogen gas (heater temperature 250 °C) at a constant flow rate of 10 L/min. The sample was diluted with methanol and injected at a constant flow rate of 0.1 mL/min. The spectrometer scanned from m/z 130 to 500.

2.8. Evaluation of cell viability after addition of polymers to the culture medium

HuH-7 or HUVEC cells were seeded in 96-well culture plates (HuH-7: 4000 cells/well, HUVEC: 5000 cells/well) and incubated overnight in 100 μL DMEM supplemented with 10% FBS and penicillin/streptomycin. After the culture medium was replaced with fresh medium containing 10% FBS, a polymer solution of P[Asp(DET)], P[Glu(DET)], LPEI or the degradation products P[Asp(DET)] obtained after incubation at 37 °C were added at varing concentration. Cell viability was determined using the Cell Counting Kit-8 (Dojindo, Kumamoto, Japan) following the manufacturer's protocol.

2.9. Polyplex formation

Each polyplex sample with a pDNA concentration of 33 μg/mL was prepared by mixing pDNA and polycation (P[Asp(DET)], P[Glu(DET)] or LPEI) at the indicated N/P ratio (=[total amines in polycation]/[DNA phosphates]) in Tris–HCl buffer solution (10 mM, pH 7.4).

2.10. Luciferase expression after transfection using polyplexes

Cells were seeded in 96-well culture plates and incubated overnight in 100 μL DMEM supplemented with 10% FBS and penicillin/streptomycin. For each transfection, the culture medium was replaced with fresh medium containing 10% FBS and then the polyplex solution was administered to each well. Firefly luciferase expression was measured with the Luciferase assay system (Promega, Madison, WI, USA) and a GloMaxTM 96 microplate luminometer (Promega) according to the manufacturer's protocol. Luciferase expressions of firefly and renilla were measured with the Dual-luciferase reporter assay system (Promega).

2.11. Housekeeping gene expression assay

After performing a similar transfection procedure as previously described, total RNA was collected after 48 h using an RNeasy Mini Preparation Kit (Qiagen, Hilden, Germany). Taqman express endogenous control plate (Applied Biosystems, Foster City, CA, USA) was used to evaluate the expression of 31 endogenous housekeeping genes and 18S rRNA. The expression of each gene was normalized by the expression of 18S rRNA, and the data were expressed as relative values to the control cells without transfection.

2.12. Evaluation of cytokine induction after in vivo administration of polymers

Mice were anesthetized with isoflurane inhalation, and then 300 μL of polymer solution containing 0.79 μmol amine was injected intraperitoneally. This amine dose corresponded to that used for complexing 50 μg pDNA. After 4 h of injection, the whole blood was collected from inferior vena cava and left overnight at 4 °C. Samples were centrifuged and the supernatants were harvested for serum. Serum concentrations of IL-6 and TNF-α were measured by Quantikine colorimetric sandwich ELISA kits (R&D Systems, Minneapolis, MN, USA), following the manufacturer's instructions.

3. Results

3.1. Biodegradability of P[Asp(DET)] and P[Glu(DET)]

To evaluate the biodegradability of P[Asp(DET)], GPC measurements were performed after incubating P[Asp(DET)] (pH 7.4) at 37 °C. As shown in Fig. 2A, P[Asp(DET)] showed considerable degradation even after one-day incubation which progressed gradually. When the degradation products formed in the solution at pH 7.4 were analyzed by ESI-MS, most of the detectable signals were in good agreement with masses of Asp(DET) monomer and its oligomers (Fig. 3). This suggested that degradation occurred due to selective backbone cleavage of P[Asp(DET)].

The facile degradability of N-substituted polyaspartamides has been previously reported, although the exact mechanism remained unclear [12]. An asparagine (Asn) residue in peptides and proteins is known to induce non-enzymatic deamidation under physiological conditions, which results in the rearrangement of Asn to Asp while releasing NH_3 [13–17]. In this reaction, five-member succinimide intermediate formation plays an important role [14].

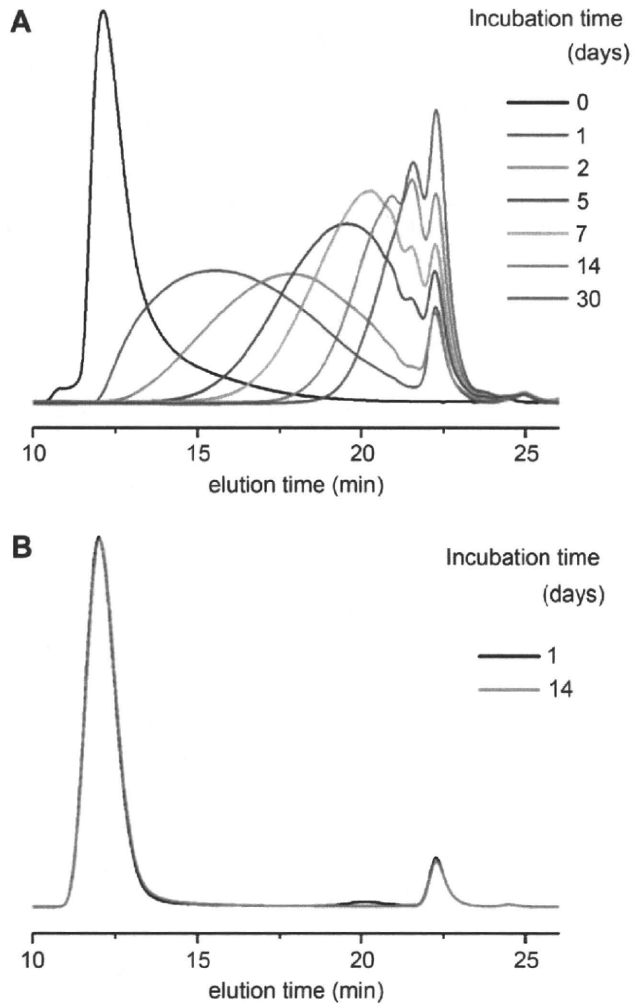

Fig. 2. GPC profiles during time-course degradation of P[Asp(DET)] (A) and P[Glu(DET)] (B) in phosphate buffer solution (10 mM, pH 7.4) containing 150 mM NaCl at 37 °C.

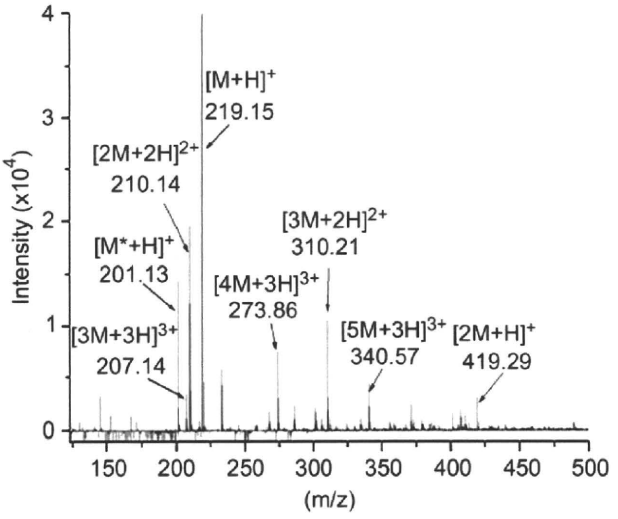

Fig. 3. ESI-MS spectrum of degraded P[Asp(DET)]. The sample was incubated as an aqueous solution (pH 7) at 37 °C for one month. M: estimated molecular mass of Asp(DET) and isomerized Asp(DET), M*: estimated molecular mass of Asp(DET) as a five-membered ring intermediate.

Although succinimide formation of Asn primarily occurs via a nucleophilic attack of the amide nitrogen backbone on the side-chain carbonyl (Fig. 4 pathway (a)), cleavage of the backbone at an Asn residue in peptides and proteins has also been reported, where succinimide formation occurred via a nucleophilic attack of a side-chain amide nitrogen on the backbone carbonyl (Fig. 4 pathway (b)) [13,15,17]. Thus, it is reasonable to assume that five-membered succinimide formation played an important role in the cleavage of the PAsp backbone.

Then, we synthesized a derivative polymer, N-substituted polyglutamide (P[Glu(DET)]), as a comparative gene carrier (Fig. 1). Although an N-substituted polyglutamide can also form a six-membered cyclic imide in similar mechanism as P[Asp(DET)], the conformation has less favorable geometry [15,18]. As expected, P[Glu(DET)] showed no degradation, even after a two-week incubation at 37 °C (Fig. 2B). It should be noted that these two polymers possess an identical DET side chain, which has been shown to have an excellent gene transfection efficiency, as described in the Introduction section. Thus, by comparing these two polymers, we could analyze the biological functions specifically related to the degradabilities of these polymers.

3.2. Polymer degradability in maintaining cellular homeostasis

We hypothesized that degradability of a polymer would play an important role in achieving safe and sustained transgene expression. First, we evaluated cell viability in the presence of polymers in the culture medium. The intact polymer of P[Asp(DET)], P[Glu(-DET)], LPEI, or the degradation products of P[Asp(DET)] were added to the culture medium at varying concentrations. As shown in Fig. 5, the intact polymers showed cytotoxicity in a manner dependent on the concentration of amines, where an amine concentration of >0.04 mM (HuH-7) or 0.01 mM (HUVEC) resulted in decreased cell viability. In contrast, the degradation products of P[Asp(DET)] collected after incubation at 37 °C resulted in less cytotoxicity. In particular, using the degradation products after incubation for two or more days, no cytotoxicity was evident, even at high concentrations of amines (up to 1 mM).

Next, we evaluated the transfection efficiency of cultured cells. To focus on cell conditions and transgene expression, we used HuH-7 cells that stably expressed firefly luciferase and evaluated the fluctuations in endogenous firefly expression and transfected renilla luciferase expression. In preliminary experiments, transfection with single administration of polyplexes followed by the

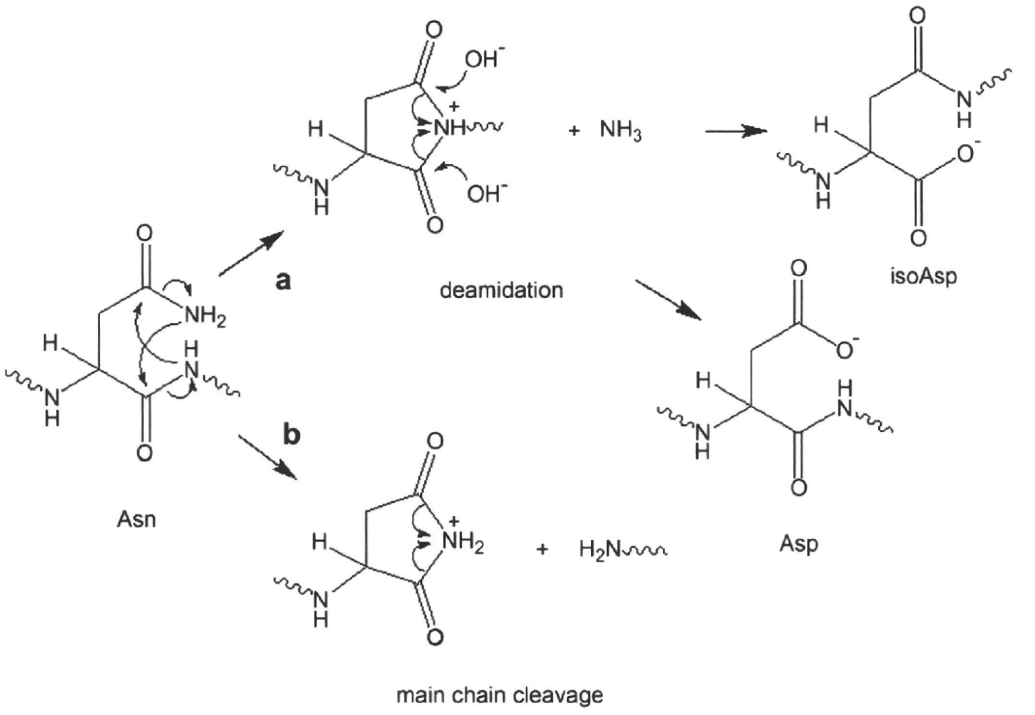

Fig. 4. Pathway for spontaneous deamidation of Asn, followed by isomerization of Asp (a) and backbone cleavage by an asparagine residue in polypeptides (b).

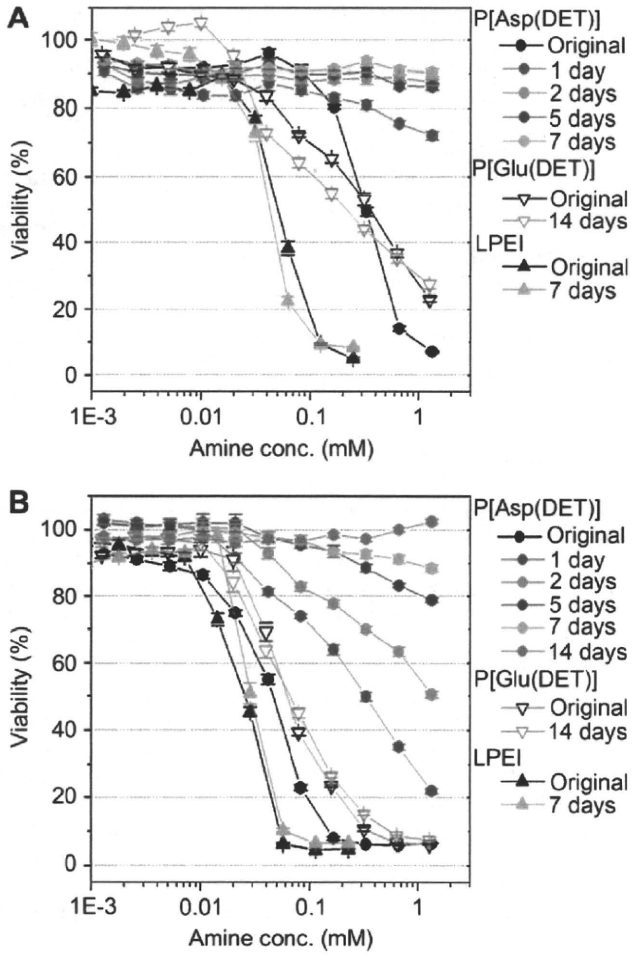

Fig. 5. Cell viability after addition of P[Asp(DET)], P[Glu(DET)], LPEI, or the degradation products of P[Asp(DET)]. HuH-7 (A) or HUVEC (B) cells were incubated in the presence of these compounds at varying concentrations and their viabilities were evaluated after 48 h.

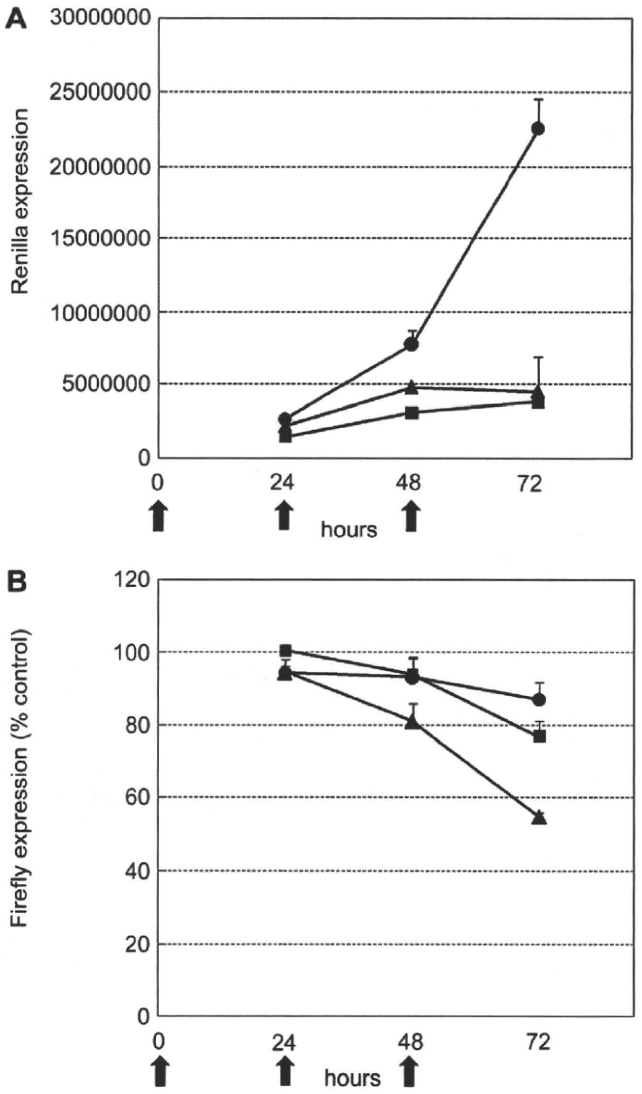

Fig. 6. Repeated transfections by pDNA encoding renilla luciferase in HuH-7 cells that stably expressed firefly luciferase. Both renilla (A) and firefly (B) luciferase expressions were evaluated simultaneously at defined time points. Arrows indicate the time of transfection set at every 24 h. Closed circles, squares and triangles represent expressions of P[Asp(DET)], P[Glu(DET)], and LPEI, respectively. Each data represents mean ± SEM (n = 6).

measurement of luciferase expressions after 24 and 48 h showed minimal differences among polymers of P[Asp(DET)], P[Glu(DET)], and LPEI at optimal N/P conditions (data not shown). To highlight the effects of the degradability of polymer on cells, we performed repeated transfections by administering polyplexes for every 24 h with refreshing of the culture medium. For this case, a polyplex solution formed at N/P = 5 with 0.25 μg pDNA was added to each well in a 96-well culture plate filled with 100 μL culture medium. Using these conditions, the final amine concentration corresponded to 0.04 mM in the medium, which would not have cytotoxic effects, even in the intact polymer form according to the results in Fig. 5.

As shown in Fig. 6A, P[Asp(DET)] resulted in a continuous increase in renilla expression until 72 h after repeated transfections for every 24 h using polyplex administration. Endogenous firefly luciferase expression remained constant during this time period (Fig. 6B). In contrast, using P[Glu(DET)], or LPEI, the renilla expression leveled off at 48 h after first transfection in parallel with the gradual down-regulation of endogenous firefly expression. Interestingly, the renilla expressions at 24 h post-transfection were comparable among polymers. Thus, these results suggest that, although a single dose of each polyplex caused minimal toxic effects on HuH-7 cells, repeated transfections resulted in cumulative toxicity when using the non-degradable polymers of P[Glu(DET)] and LPEI. By comparison, P[Asp(DET)] caused minimal cytotoxicity as P[Asp(DET)] was rapidly degraded to a non-toxic form.

HUVECs were also used for repeated transfections. Primary cells, such as HUVEC, are apt to be sensitive to the toxicity caused by cationic polymers. Indeed, as shown in Fig. 5B, the critical concentration of amines in the intact polymers that showed cytotoxicity to HUVEC was 0.01 mM, which was ¼ lower than for HuH-7 cells (0.04 mM). Thus, for these assays using HUVECs, a ¼ lower dose of polyplex prepared at N/P = 5 was applied. As shown in Fig. 7, P[Asp(DET)] showed a similar tendency with HuH-7 for a continuous increase in the luciferase expression during 72 h, whereas P[Glu(DET)] and LPEI showed decreases after 48 h of transfection.

For a detailed investigation focusing on cellular homeostasis, we analyzed the fluctuations in gene expressions of 31 frequently used housekeeping genes after transfections using P[Asp(DET)] or P[Glu(DET)]. These genes usually show uniform expressions,

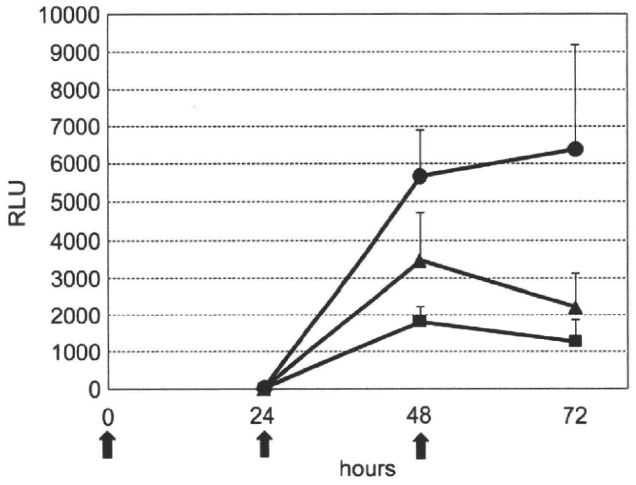

Fig. 7. Luciferase expression in HUVEC after repeated transfection. Arrows indicate the time of transfection set at every 24 h. Closed circles, squares and triangles represent expressions of P[Asp(DET)], P[Glu(DET)], and LPEI, respectively. Each data represents mean ± SEM (n = 6).

although their expression profiles may vary in response to various external stimuli, such as cell stress [19]. Thus, variations in their expression profiles are good indicators for assessing cellular function, which reflect possible perturbations in cellular homeostasis. As shown in Fig. 8, all genes evaluated after transfection using P[Asp(DET)] remained within a 2-fold fluctuation compared to control cells. In contrast, P[Glu(DET)] induced larger fluctuations in the gene expressions, suggesting greater effects that altered the expressions of endogenous genes. Although the detailed mechanisms within cells should be investigated further, these results strongly suggest that P[Asp(DET)] maintained cellular homeostasis during the processes of transgene expression.

3.3. Cytokine induction after in vivo intraperitoneal injection

Finally, to evaluate the feasibility of P[Asp(DET)] biodegradability for clinical uses, we analyzed cytokine induction using *in vivo* experiments. Polymers were injected interperitoneally and serum concentrations of IL-6 and TNF-α were measured by ELISA after 4 h of injection. As shown in Fig. 9, the degradation products of P[Asp(DET)] induced these cytokines only to an extent comparable to normal saline, whereas the intact polymers induced detectable cytokine production. Considering the cationic nature of these polymers that could cause acute responses in the body, it may be difficult to completely eliminate cytokine induction after administration. However, these results indicate that once P[Asp(DET)] is degraded in the body it would cause almost no toxic reactions in a cumulative manner.

4. Discussion

In this study, we demonstrated that the biodegradability of P[Asp(DET)] contributed significantly to its safe and excellent transfection efficiency. *In vitro* evaluations of cytotoxicity due to the presence of polymers in the culture medium and by measurements of inflammatory cytokines after *in vivo* injection of polymers revealed that the degradation products of P[Asp(DET)] had almost no toxic effects on cells and tissues. Thus, P[Asp(DET)] has a clear advantage over other polymers as it can minimize the toxicity developed because of such polymers remaining within cells or in the body. Moreover, it is strongly suggested that the biodegradability of P[Asp(DET)] played an important role in maintaining cellular homeostasis after transgene expression in comparison with a non-degradable derivative polymer, P[Glu(DET)]. Because these two polymers possess identical amine units on their side chains, they showed similar properties of transgene expression and cytotoxicity just after the initial transfection (Day 1). However, on subsequent days, pharmacogenomic analysis showed remarkable differences in cell behavior, which ultimately affects long-term transgene expression. This type of cumulative toxicity observed

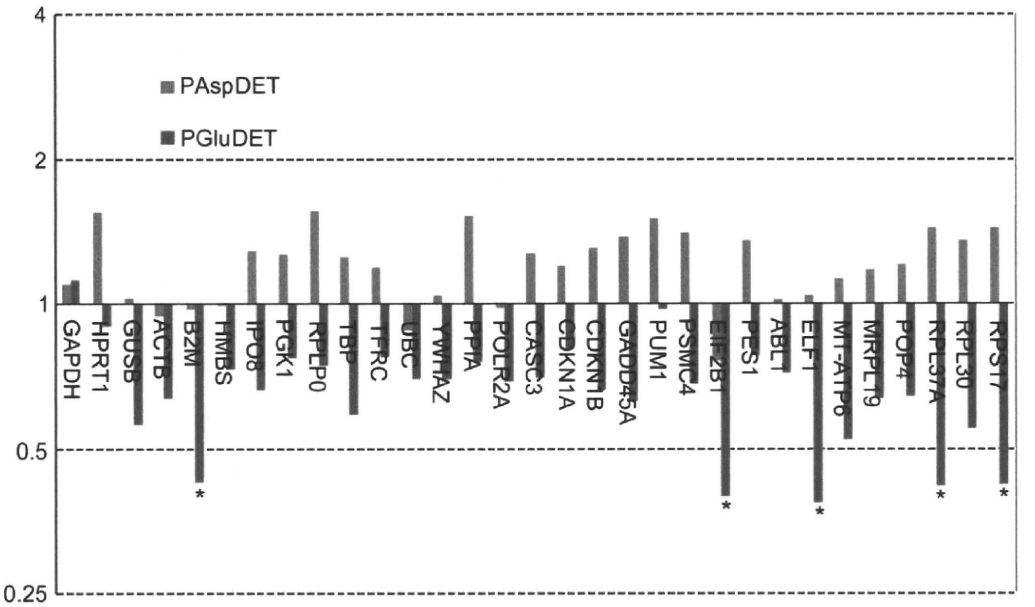

Fig. 8. Expression profiles of endogenous housekeeping genes in HUVEC after transfection using P[Asp(DET)] or P[Glu(DET)]. 31 genes were evaluated after 48 h of transfection using a Taqman express endogenous control plate. Asterisks indicate genes showing more than 2-fold fluctuation.

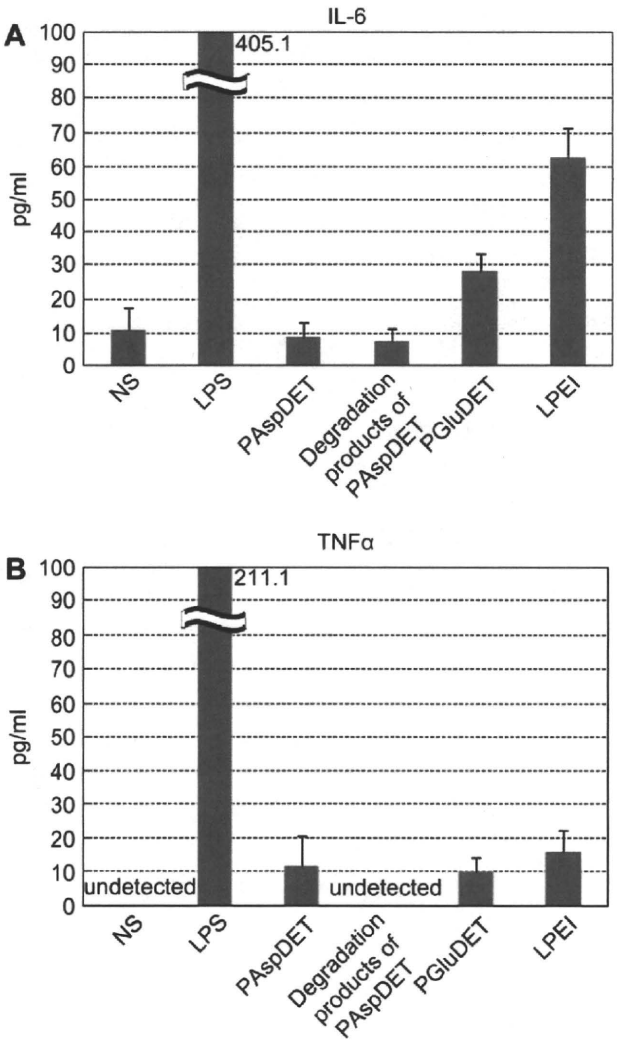

Fig. 9. Cytokine induction after intraperitoneal injection of polymers. Serum concentrations of IL-6 (A) and TNF-α (B) were measured after 4 h of injection of P[Asp(DET)], P[Glu(DET)], LPEI or the degradation products of P[Asp(DET)]. LPS was used as a positive control for measurements. Each data represents mean ± SEM (n = 4).

with P[Glu(DET)] requires careful consideration when gene introduction is applied to regulate cell function and differentiation. For example, the production of induced pluripotent stem (iPS) cells by gene introductions of Oct3/4, Sox2, Klf4, and/or c-Myc using commercially available non-viral systems have been reported. However, unlike a retrovirus, repeated administrations on each day or at an interval of few days were required to obtain sufficient expressions of these factors in a sustained manner [20,21]. Because transgene expression obtained using non-viral carriers is primarily transient, repeated administrations of gene carriers are essential for applications like stem cell engineering. In this regard, the biodegradability of P[Asp(DET)] provides it with a clear advantage to be used clinically by minimizing cumulative toxicity caused by polymers remaining within cells or in the body.

It is interesting that P[Asp(DET)] and P[Glu(DET)] showed remarkable differences in their biodegradabilities due to the presence of an extra methylene group in the Glu backbone. As described briefly in the Results section, this phenomenon may be attributed to the entropically more favorable formation of a five-membered cyclic imide as compared with a six-membered cyclic imide. In natural peptides and proteins, succinimide formation by Asn mostly occurs via a nucleophilic attack of the amide nitrogen backbone on the side-chain carbonyl, followed by non-enzymatic deamidation. This results in occasional cleavage of the backbone, which has been estimated to be less than 10% of the deamidation [15]. Nevertheless, in this study, after one-month incubation of P[Asp(DET)] under physiological conditions, no fragments containing a deamidated Asp residue were identified by ESI-MS analysis (Fig. 3). After incubation for three months, final fragments corresponded to Asp(DET) monomer (Supplemental Fig. S3), indicating that selective cleavage of the backbone occurred in P[Asp(DET)] due to the increased nucleophilicity of the side-chain amide nitrogen. To be noted is that the degradation of P[Asp(DET)] was nearly restricted in a lower temperature (i.e., 4 °C) (Supplemental Fig. S4), which provides an advantage during purification, storage, and manipulation. The detailed mechanism of the backbone cleavage in N-substituted polyaspartamides is now under investigation and will be reported in the near future.

5. Conclusion

In this study, we demonstrated that facile degradability of P[Asp(DET)] to a non-toxic form under physiological conditions played an important role in its use as an effective gene carrier. Its degradation was induced by the cleavage of the PAsp backbone due to the self-catalytic reaction between the backbone and the side-chain amide nitrogen. In comparison with a non-degradable derivative polymer, P[Glu(DET)], P[Asp(DET)] achieved high and sustained transgene expression without affecting cellular homeostasis, which is of great importance as a practical system for non-viral gene introduction.

Acknowledgements

This work was financially supported in part by the Core Research Program for Evolutional Science and Technology (CREST) from Japan Science and Technology Corporation (JST) (K.K.), Grants-in-Aid for Scientific Research from the Japanese Ministry of Education, Culture, Sports, Science and Technology (K.I.), and Medical Research Grant on Traffic Accident from the General Insurance Association of Japan (K.I.). We appreciate Prof. Masaru Kato (The University of Tokyo) for kind help in the ESI-MS measurements. We also thank Ms. Satomi Ogura (The University of Tokyo) for technical assistance.

Appendix

Figures with essential colour discrimination. Certain figures in this article, in particular Figs. 2 and 8 may be difficult to interpret in black and white. The full colour images can be found in the on-line version, at doi:10.1016/j.biomaterials.2009.11.072.

Appendix. Supplementary information

Supplementary data associated with this article can be found, in the online version, at doi:10.1016/j.biomaterials.2009.11.072.

References

[1] De Smedt SC, Demeester J, Hennink WE. Cationic polymer based gene delivery systems. Pharm Res 2000;17:113–26.
[2] Schaffert D, Wagner E. Gene therapy progress and prospects: synthetic polymer-based systems. Gene Ther 2008;15:1131–8.
[3] Itaka K, Kataoka K. Recent development of nonviral gene delivery systems with virus-like structures and mechanisms. Eur J Pharm Biopharm 2009;71:475–83.

[4] Boussif O, Lezoualc'h F, Zanta MA, Mergny MD, Scherman D, Demeneix B, et al. A versatile vector for gene and oligonucleotide transfer into cells in culture and in vivo: polyethylenimine. Proc Natl Acad Sci U S A 1995;92:7297–301.
[5] Kanayama N, Fukushima S, Nishiyama N, Itaka K, Jang WD, Miyata K, et al. A PEG-based biocompatible block catiomer with high buffering capacity for the construction of polyplex micelles showing efficient gene transfer toward primary cells. Chem Med Chem 2006;1:439–44.
[6] Masago K, Itaka K, Nishiyama N, Chung UI, Kataoka K. Gene delivery with biocompatible cationic polymer: pharmacogenomic analysis on cell bioactivity. Biomaterials 2007;28:5169–75.
[7] Akagi D, Oba M, Koyama H, Nishiyama N, Fukushima S, Miyata T, et al. Biocompatible micellar nanovectors achieve efficient gene transfer to vascular lesions without cytotoxicity and thrombus formation. Gene Ther 2007;14:1029–38.
[8] Itaka K, Ohba S, Miyata K, Kawaguchi H, Nakamura K, Takato T, et al. Bone regeneration by regulated in vivo gene transfer using biocompatible polyplex nanomicelles. Mol Ther 2007;15:1655–62.
[9] Harada-Shiba M, Takamisawa I, Miyata K, Ishii T, Nishiyama N, Itaka K, et al. Intratracheal gene transfer of adrenomedullin using polyplex nanomicelles attenuates monocrotaline-induced pulmonary hypertension in rats. Mol Ther 2009;17:1180–6.
[10] Miyata K, Oba M, Nakanishi M, Fukushima S, Yamasaki Y, Koyama H, et al. Polyplexes from poly(aspartamide) bearing 1,2-diaminoethane side chains induce pH-selective, endosomal membrane destabilization with amplified transfection and negligible cytotoxicity. J Am Chem Soc 2008;130:16287–94.
[11] De Marre A, Soyez H, Schacht E, Pytela J. Improved method for the preparation of poly[N5-(2-hydroxyethyl)-L-glutamine] by aminolysis of poly(γ-benzyl-L-glutamate). Polymer 1994;35:2443–6.
[12] Neuse E, Perlwitz A, Schmitt S. Water-soluble polyamides as potential drug carrier, III. Relative main-chain stabilities of side chain-functionalized aspartamide polymers on aqueous-phase dialysis. Die Angewandte Makromolekulare Chemie 1991;192:35–50.
[13] Geiger T, Clarke S. Deamidation, isomerization, and racemization at asparaginyl and aspartyl residues in peptides. Succinimide-linked reactions that contribute to protein degradation. J Biol Chem 1987;262:785–94.
[14] Johnson BA, Shirokawa JM, Hancock WS, Spellman MW, Basa LJ, Aswad DW. Formation of isoaspartate at two distinct sites during in vitro aging of human growth hormone. J Biol Chem 1989;264:14262–71.
[15] Wright HT. Nonenzymatic deamidation of asparaginyl and glutaminyl residues in proteins. Crit Rev Biochem Mol Biol 1991;26:1–52.
[16] Tyler-Cross R, Schirch V. Effects of amino acid sequence, buffers, and ionic strength on the rate and mechanism of deamidation of asparagine residues in small peptides. J Biol Chem 1991;266:22549–56.
[17] Liu DT. Deamidation: a source of microheterogeneity in pharmaceutical proteins. Trends Biotechnol 1992;10:364–9.
[18] Bernard T, Joachim MM. The hydrolysis of peptides. In: Hydrolysis in drug and prodrug metabolism. Wiley-VCH; 2003. p. 236–358.
[19] Thellin O, Zorzi W, Lakaye B, De Borman B, Coumans B, Hennen G, et al. Housekeeping genes as internal standards: use and limits. J Biotechnol 1999;75:291–5.
[20] Okita K, Nakagawa M, Hyenjong H, Ichisaka T, Yamanaka S. Generation of mouse induced pluripotent stem cells without viral vectors. Science 2008;322:949–53.
[21] Gonzalez F, Barragan Monasterio M, Tiscornia G, Montserrat Pulido N, Vassena R, Batlle Morera L, et al. Generation of mouse-induced pluripotent stem cells by transient expression of a single nonviral polycistronic vector. Proc Natl Acad Sci U S A 2009;106:8918–22.

molecular pharmaceutics

articles

Antiangiogenic Gene Therapy of Solid Tumor by Systemic Injection of Polyplex Micelles Loading Plasmid DNA Encoding Soluble Flt-1

Makoto Oba,[†] Yelena Vachutinsky,[‡] Kanjiro Miyata,[§] Mitsunobu R. Kano,[∥,⊥] Sorato Ikeda,[#] Nobuhiro Nishiyama,*[,§] Keiji Itaka,[§] Kohei Miyazono,[∥,⊥] Hiroyuki Koyama,[†] and Kazunori Kataoka*[,‡,§,∥,#]

Department of Clinical Vascular Regeneration, Graduate School of Medicine, The University of Tokyo, 7-3-1 Hongo, Bunkyo, Tokyo 113-8655, Japan, Department of Bioengineering, Graduate School of Engineering, The University of Tokyo, 7-3-1 Hongo, Bunkyo, Tokyo 113-8656, Japan, Center for Disease Biology and Integrative Medicine, Graduate School of Medicine, The University of Tokyo, 7-3-1 Hongo, Bunkyo, Tokyo 113-0033, Japan, Center for NanoBio Integration, The University of Tokyo, 7-3-1 Hongo, Bunkyo, Tokyo 113-8656, Japan, Department of Molecular Pathology, Graduate School of Medicine, The University of Tokyo, 7-3-1 Hongo, Bunkyo-ku, Tokyo 113-8655, Japan, and Department of Materials Engineering, Graduate School of Engineering, The University of Tokyo, 7-3-1 Hongo, Bunkyo, Tokyo 113-8656, Japan

Received September 14, 2009; Revised Manuscript Received January 8, 2010; Accepted February 23, 2010

Abstract: In this study, a polyplex micelle was developed as a potential formulation for antiangiogenic gene therapy of subcutaneous pancreatic tumor model. Poly(ethylene glycol)-poly(L-lysine) block copolymers (PEG-PLys) with thiol groups in the side chain of the PLys segment were synthesized and applied for preparation of disulfide cross-linked polyplex micelles through ion complexation with plasmid DNA (pDNA) encoding the soluble form of vascular endothelial growth factor (VEGF) receptor-1 (sFlt-1), which is a potent antiangiogenic molecule. Antitumor activity and gene expression of polyplex micelles with various cross-linking rates were evaluated in mice bearing subcutaneously xenografted BxPC3 cell line, derived from human pancreatic adenocarcinoma, and polyplex micelles with optimal cross-linking rate achieved effective suppression of tumor growth. Significant gene expression of this micelle was detected selectively in tumor tissue, and its antiangiogenic effect was confirmed by decreased vascular density inside the tumor. Therefore, the disulfide cross-linked polyplex micelle loading sFlt-1 pDNA has a great potential for antiangiogenic therapy against subcutaneous pancreatic tumor model by systemic application.

Keywords: Polymeric micelle; block copolymer; antiangiogenic tumor gene therapy; sFlt-1

Introduction

Antiangiogenic tumor gene therapy is an intensively studied approach to inhibit tumor growth by destructing its neo-vasculature formation.[1,2] Vascular endothelial growth factor (VEGF) is a major proangiogenic molecule, which stimulates angiogenesis via promoting endothelial prolifera-

* To whom correspondence should be addressed. K.K.: tel, +81-3-5841-7138; fax, +81-3-5841-7139; e-mail, kataoka@bmw.t.u-tokyo.ac.jp; The University of Tokyo, Department of Materials Engineering, 7-3-1 Hongo, Bunkyo-ku, Tokyo 113-8656, Japan. N.N.: tel, +81-3-5841-1430; fax, +81-5841-7139; e-mail, nishiyama@bmw.t.u-tokyo.ac.jp.

† Department of Clinical Vascular Regeneration, Graduate School of Medicine.

‡ Department of Bioengineering, Graduate School of Engineering.

§ Center for Disease Biology and Integrative Medicine, Graduate School of Medicine.

∥ Center for NanoBio Integration.

⊥ Department of Molecular Pathology, Graduate School of Medicine.

Department of Materials Engineering, Graduate School of Engineering.

10.1021/mp9002317 © 2010 American Chemical Society
Published on Web 02/23/2010

tion, survival, and migration. The soluble form of VEGF receptor-1 (fms-like tyrosine kinase-1: Flt-1) is a potent endogeneous molecule, which can be used for antiangiogenic therapy.[3,4] The sFlt-1 binds to VEGF with the same affinity and equivalent specificity as that of the original receptor,[5] however it inhibits its signal transduction.

Gene therapy is becoming a promising strategy to supply consecutive expression of antiangiogenic proteins over a period of time. Indeed, a number of studies have already demonstrated the potential of therapeutic genes encoding angiogenic inhibitors to suppress tumor growth.[6,7] The major challenge in systemic gene therapy, however, is a need for a safe and effective vector system that can deliver the gene to the target tissue and cells with no detrimental side effects. In terms of safety, nonviral gene vectors are gaining popularity over viral vectors, however, their intracellular delivery and transfection potential require further optimization. Recently, several reports were published on *in vivo* nonviral gene therapy utilizing sFlt-1 for inhibition of tumor angiogenesis.[8,9]

Based on these criteria, cross-linked polyplex micelles were designed and prepared through electrostatic interaction of thiolated poly(ethylene glycol)-poly(L-lysine) (PEG-PLys) block copolymers and plasmid DNA (pDNA) encoding sFlt-1. We have previously reported that disulfide cross-links introduced into the polyplex micelle core contribute to the stabilization of its structure in the extracellular entity while facilitating smooth release of the entrapped pDNA, in response to the reductive environment, inside the cells.[10,11] The outer hydrophilic shell layer, formed by PEG segment, increases complex stability in serum, avoiding nonspecific interactions with plasma proteins and reduces polymer toxicity.[12]

In this study, cross-linked polyplex micelles were systemically administered to mice bearing subcutaneously xenografted BxPC3 human pancreatic adenocarcinoma and evaluated for their transfection efficiency. Note that BxPC3 xenografts, as some intractable solid tumors, are characterized by stroma-rich histology,[13] which limits access of therapeutic agents to tumor cells. Thus, the accessibility of endothelial cells by bloodstream makes an antiangiogenic approach an attractive strategy against this model. Here we report a potent tumor growth inhibitory effect achieved by effective antiangiogenic ability by the polyplex micelles with an optimal cross-linking degree, which enables the selective expression of loaded sFlt-1 gene in tumor tissue.

Experimental Section

Materials. pDNA for luciferase (Luc) with the pCAcc vector having the CAG promoter was provided by RIKEN Gene Bank (Tsukuba, Japan) and amplified in competent DH5α *Escherichia coli*, followed by purification using a NucleoBond Xtra Maxi (Machery-Nagel GmbH & Co. KG, Düren, Germany). Dulbecco's modified Eagle's medium (DMEM) and RPMI 1640 medium were purchased from Sigma-Aldrich Co. (Madison, WI). Fetal bovine serum (FBS) was purchased from Dainippon Sumitomo Pharma Co., Ltd. (Osaka, Japan). Alexa488- and Alexa647-conjugated secondary antibodies to rat IgG were obtained from Invitrogen Molecular Probes (Eugene, OR). Human soluble VEGF R1/

(1) Folkman, J. Tumor Angiogenesis: Therapeutic Implications. *N. Engl. J. Med.* **1971**, *285*, 1182–1186.
(2) Quesada, A. R.; Munoz-Chapuli, R.; Medina, M. A. Anti-angiogenic Drugs: from Bench to Clinical Trials. *Med. Res. Rev.* **2006**, *26*, 483–530.
(3) Shibuya, M.; Yamaguchi, S.; Yamane, A.; Ikeda, T.; Tojo, A.; Matsushime, H.; Sato, M. Nucleotide Sequence and Expression of a Novel Human Receptor-type Tyrosine Kinase Gene (flt) Closely Related to the Fms Family. *Oncogene* **1990**, *5*, 519–524.
(4) Kendall, R. L.; Thomas, K. A. Inhibition of Vascular Endothelial Cell Growth Factor Activity by an Endogenously Encoded Soluble Receptor. *Proc. Natl. Acad. Sci. U.S.A.* **1993**, *90*, 10705–10709.
(5) Kendall, R. L.; Wang, G.; Thomas, K. A. Identification of a Natural Soluble Forma of the Vascular Endothelial Growth Factor Receptor, FLT-1, and Its Heterodimerization with KDR. *Biochem. Biophys. Res. Commun.* **1996**, *226*, 324–428.
(6) Kong, H. L.; Hecht, D.; Song, W.; Kovesdi, I.; Hackett, N. R.; Yayon, A.; Crystal, R. G. Regional Suppression of Tumor Growth by In Vivo Transfer of a cDNA Encoding a Secreted form of the Extracellular Domain of the Flt-1 Vascular Endothelial Growth Factor Receptor. *Hum. Gene Ther.* **1998**, *9*, 823–833.
(7) Kuo, C. J.; Farnebo, F.; Yu, E. Y.; Christofferson, R.; Swearingen, R. A.; Charter, R.; von Recum, H. A.; Yuan, J.; Kamihara, J.; Flynn, E.; D' Amato, R.; Folkman, J.; Mulligan, R. C. Comparative Evaluation of the Antitumor Activity of Antiangiogenic Proteins Delivered by Gene Transfer. *Proc. Natl. Acad. Sci. U.S.A.* **2001**, *98*, 4605–4610.
(8) Kim, W. J.; Yockman, J. W.; Jeong, J. H.; Christensen, L. V.; Lee, M.; Kim, Y. H.; Kim, S. W. Anti-angiogenic Inhibition of Tumor Growth by Systemic Delivery of PEI-g-PEG-RGD/pCMV-sFlt-1 Complexes in Tumor-bearing Mice. *J. Controlled Release* **2006**, *114*, 381–388.
(9) Kommareddy, S.; Amiji, M. Antiangiogenic Gene Therapy with Systemically Administered sFlt-1 Plasmid DNA in Engineered Gelatin-based Nanovactors. *Cancer Gene Ther.* **2007**, *14*, 488–498.
(10) Miyata, K.; Kakizawa, Y.; Nishiyama, N.; Harada, A.; Yamasaki, Y.; Koyama, H.; Kataoka, K. Block Catiomer Polyplexes with Regulated Densities of Charge and Disulfide Cross-linking Directed to Enhance Gene Expression. *J. Am. Chem. Soc.* **2004**, *126*, 2355–2361.
(11) Miyata, K.; Kakizawa, Y.; Nishiyama, N.; Yamasaki, Y.; Watanabe, T.; Kohara, M.; Kataoka, K. Freeze-dried Formulations for *In Vivo* Gene Delivery of PEGylated Polyplex Micelles with Disulfide Crosslinked Cores to the Liver. *J. Controlled Release* **2005**, *109*, 15–23.
(12) Itaka, K.; Yamauchi, K.; Harada, A.; Nakamura, K.; Kawaguchi, H.; Kataoka, K. Polyion Complex Micelles from Plasmid DNA and Poly(ethylene glycol)-poly(L-lysine) Block Copolymer as Serum-tolerable Polyplex System: Physicochemical Properties of Micelles Relevant to Gene Transfection Efficiency. *Biomaterials* **2003**, *24*, 4495–4506.
(13) Kano, M. R.; Bae, Y.; Iwata, K.; Morishita, Y.; Yashiro, M.; Oka, M.; Fujii, T.; Komuro, A.; Kiyono, K.; Kaminishi, M.; Hirakawa, K.; Ouchi, Y.; Nishiyama, N.; Kataoka, K.; Miyazono, K. Improvement of Cancer-targeting Therapy, Using Nanocarriers for Intractable Solid Tumors by Inhibition of TGF-beta Signaling. *Proc. Natl. Acad. Sci. U.S.A.* **2007**, *104*, 3460–3465.

Flt-1 immunoassay kit was purchased from R&D Systems, Inc. (Minneapolis, MN). Gemcitabine was obtained from Eli Lilly and Company (Indianapolis, IN). Avastin was obtained from F. Hoffmann-La Roche, Ltd. (Basel, Switzerland). Synthesis of thiolated block copolymer, and construction and confirmation of pDNA encoding sFlt-1 are shown in the Supporting Information. A block copolymer with *X*% of thiolation degree was abbreviated as "B-SH*X*%".

Cell Lines and Animals. Human embryonic kidney 293T cells (from RIKEN CELL BANK, Tsukuba, Japan) and human pancreatic adenocarcinoma BxPC3 cells (from ATCC, Manassas, VA) were maintained in DMEM and RPMI medium, respectively, supplemented with 10% FBS in a humidified atmosphere containing 5% CO_2 at 37 °C. 293T cells were chosen for *in vitro* experiments as cells that did not express sFlt-1.[14] Balb/c nude mice (female, 5 weeks old) were purchased from Charles River Laboratories (Tokyo, Japan). All animal experimental protocols were performed in accordance with the Guide for the Care and Use of Laboratory Animals as stated by the National Institutes of Health.

Preparation of Polyplex Micelles. Each block copolymer was dissolved in 10 mM Tris-HCl buffer (pH 7.4), followed by the addition of 10-times-excess mol of dithiothreitol (DTT) against thiol groups. After 30 min incubation at room temperature, the polymer solution was added to a twice-excess volume of 225 μg/mL pDNA/10 mM Tris-HCl (pH 7.4) solution to form polyplex micelles with N/P ratio = 2. Note that N/P ratio was defined as the residual molar ratio of amino groups of thiolated PEG-PLys to phosphate groups of pDNA. The final pDNA concentration was adjusted to 150 μg/mL. After overnight incubation at room temperature, the polyplex micelle solution was dialyzed against 10 mM Tris-HCl buffer (pH 7.4) containing 0.5 vol% DMSO at 37 °C for 24 h to remove the impurities, followed by 24 h of additional dialysis against 10 mM Tris-HCl buffer (pH 7.4) or 10 mM Hepes buffer (pH 7.4) to remove DMSO. During the dialysis, the thiol groups of thiolated block copolymers were oxidized to form disulfide cross-links. In the *in vivo* experiments, the polyplex micelle solution was adjusted to a concentration of 100 μg of pDNA/mL in 10 mM Hepes buffer (pH 7.4) with 150 mM NaCl.

Dynamic Light Scattering (DLS) Measurement. The size of the polyplex micelles was evaluated by DLS using Nano ZS (ZEN3600, Malvern Instruments, Ltd., U.K.). A He−Ne ion laser (633 nm) was used as the incident beam. Polyplex micelle solutions with N/P = 2 from 3 different batches were adjusted to a concentration of 33.3 μg of pDNA/mL in 10 mM Tris-HCl buffer (pH 7.4). The data obtained at a detection angle of 173° and a temperature of 37 °C were analyzed by a cumulant method to obtain the hydrodynamic diameters and polydispersity indices (μ/Γ^2) of micelles.

Zeta-Potential Measurement. The zeta-potential of polyplex micelles was evaluated by the laser-Doppler electrophoresis method using Nano ZS with a He−Ne ion laser (633 nm). Polyplex micelle solutions with N/P = 2 from 3 different batches were adjusted to a concentration of 33.3 μg pDNA/mL in 10 mM Tris-HCl buffer (pH 7.4). The zeta-potential measurements were carried out at 37 °C. A scattering angle of 173 °C was used in these measurements.

Real-Time Gene Expression. 293T cells (100,000 cells) were seeded on a 35 mm dish and incubated overnight. After replacement with fresh medium containing 0.1 mM D-luciferin, each type of polyplex micelle (N/P = 2) containing 3 μg of Luc pDNA was added. The dishes were set in a luminometer incorporated in a CO_2 incubator (AB-2550 Kronos Dio, ATTO, Tokyo, Japan), and the bioluminescence was monitored every 10 min with an exposure time of 1 min. Reproducibility was confirmed by triplicate experiments.

Antitumor Activity Assay. Balb/c nude mice were inoculated subcutaneously with BxPC3 cells (5×10^6 cells in 100 μL of PBS). Tumors were allowed to grow for 2−3 weeks to reach the proliferative phase (the size of the tumors at this point was approximately 60 mm^3). Subsequently, polyplex micelles (20 μg of pDNA/mouse), gemcitabine (100 mg/kg), or Avastin (50 mg/kg) maintained in 10 mM Hepes buffer (pH 7.4) with 150 mM NaCl were injected via the tail vein either 3 times (Figure 2a) or 5 times (Figure 2b) at 4-day intervals. Gemcitabine and Avastin doses and injection regimens were according to the previous reports published elsewhere.[15,16] A polyplex micelle containing Luc pDNA was used as a control formulation containing the nontherapeutic gene. Tumor size was measured every second day by a digital vernier caliper across its longest (a) and shortest diameters (b), and its volume (V) was calculated according to the formula $V = 0.5ab^2$.

***In Vivo* sFlt-1 Gene Expression.** Polyplex micelles loading either sFlt-1 or Luc pDNA (20 μg pDNA) were injected into the BxPC3-inoculated mice via the tail vein on days 0 and 4. Mice were sacrificed on day 6 after collecting blood, and the lungs, livers, spleens, kidneys, and tumors were excised. The excised organs were treated in 500 μL of cell culture lysis buffer (Promega, Madison, WI), homogenized, and centrifuged. The sFlt-1 concentration of supernatants was evaluated using the immunoassay kit according to the manufacturer's protocol. Note that block copolymers and polyplex micelles did not interfere with ELISA (Figure 2 in the Supporting Information).

Vascular Density in the Tumors. Polyplex micelles loading either sFlt-1 or Luc pDNA (20 μg of pDNA) and Avastin (50 mg/kg) were injected into the BxPC3-inoculated

(14) Kim, W. J.; Yockman, J. W.; Lee, M.; Jeong, J. H.; Kim, Y. H.; Kim, S. W. Soluble Flt-1 Gene Delivery Using PEI-g-PEG-RGD Conjugate for Anti-angiogenesis. *J. Controlled Release* **2005**, *106*, 224–234.

(15) Braakhuis, B. J. M.; van Dongen, G. A. M. S.; Vermorken, J. B.; Snow, G. B. Preclinical In Vivo Activity 2′,2′-Difluorodeoxycytidine (Gemcitabine) against Human Head and Neck Cancer. *Cancer Res.* **1991**, *51*, 211–214.

(16) Gerber, H. P.; Ferrara, N. Pharmacology and Pharmacodynamics of Bevacizumab as Monotherapy or in Combination with Cytotoxic Therapy in Preclinical Studies. *Cancer Res.* **2005**, *65*, 671–680.

mice via the tail vein on days 0 and 4. Mice were sacrificed on day 6, and the tumors were excised, frozen in dry-iced acetone, and sectioned at 10 μm thickness in a cryostat. Vascular endothelial cells (VECs) were immunostained by rat monoclonal antibody antiplatelet endothelial cell adhesion molecule-1 (PECAM-1) (BD Pharmingen, Franklin Lakes, NJ) and Alexa488-conjugated secondary antibody. The samples were observed with a confocal laser scanning microscope (CLSM). The CLSM observation was performed using an LSM 510 (Carl Zeiss, Oberlochen, Germany) with an EC Plan-Neoflur 20× objective (Carl Zeiss) at the excitation wavelength of 488 nm (Ar laser). The PECAM-1-positive area (%) was calculated from Alexa488-positive pixels.

***In Vivo* EGFP Gene Expression in the Tumors.** Polyplex micelles loading EGFP pDNA (20 μg of pDNA) were injected into the BxPC3-inoculated mice via the tail vein. Mice were sacrificed on either day 3 or day 7. Tumors were excised, fixed with 10% formalin, frozen, and sectioned. VECs were immunostained by anti-PECAM-1 antibody and Alexa647-conjugated secondary antibody. After nuclear staining with Hoechst 33342, CLSM observation was carried out using the LSM 510 with the EC Plan-Neoflur 20× objective at the excitation wavelength of 488 nm for EGFP expression, 633 nm (He−Ne laser) for Alexa647, and 710 nm (MaiTai laser, two photon excitation; Spectra-Physics, Mountain View, CA) for Hoechst 33342, respectively. The representative images of tumors excised on day 3 are shown in Figure 5. Note that images of tumors excised on day 7 showed similar patterns to those on day 3, however with lower intensity of EGFP expression.

Results

Formation of Polyplex Micelles. No free pDNA was detected by agarose gel electrophoresis, confirming that all pDNA was entrapped in disulfide cross-linked polyplex micelles, which were prepared as previously reported through ion complexation of block copolymers with pDNA at the N/P ratio = 2. Free thiol groups in polyplex micelles were estimated to be less than 2% by Ellman's test (data not shown), which is consistent with our previous report.[10] Weight−weight % ratios of pDNA/micelle in each formulation were as follows: 32.8% in B-SH0% formulation; 31.0% in B-SH5%; 29.2% in B-SH11%; 26.4% in B-SH20%; and 21.0% in B-SH36%. The mean size of the micelles was between 100 and 150 nm, with a moderate polydispersity index between 0.17 and 0.2 (Figure 3 in the Supporting Information), while zeta-potential revealed approximately neutral values, confirming the formation of PEG palisade surrounding the polyplex core (Table 1).

Real-Time Gene Expression. *In vitro* real-time Luc gene expression of polyplex micelles was evaluated using Kronos Dio for a prolonged period (Figure 1).[17,18] The B-SH5% cross-linked polyplex micelle showed the highest gene expression among all micelles until 60 h. Worth mentioning is that the transfection efficiency of the B-SH11% micelle continued to exceed that of the B-SH5% micelle after 60 h. Disulfide cross-links in the polyplex core are believed to contribute not only to enhanced stability of the micelles in the medium but also to sustained release of complexed pDNA inside the cells with a reductive environment, resulting in polyplex micelles with higher cross-linking rates that can maintain an appreciable transfection efficiency over a longer time scale. Note that the B-SH36% micelle showed an increasing trend in gene expression with time.

Table 1. Sizes and Zeta-Potentials of Polyplex Micelles with Various Cross-Linking Rates at N/P = 2[a]

thiolation degree (%)	cumulant diameter (nm)	polydispersity index (μ/l^{-2})	zeta-potential (mV)
0	107 ± 2	0.195 ± 0.021	1.66 ± 0.28
5	117 ± 2	0.184 ± 0.011	1.25 ± 0.40
11	116 ± 2	0.171 ± 0.013	1.02 ± 0.30
20	139 ± 6	0.182 ± 0.050	0.40 ± 0.07
36	147 ± 2	0.192 ± 0.061	−0.96 ± 0.02

[a] The results reported were expressed as mean ± SEM (n = 3).

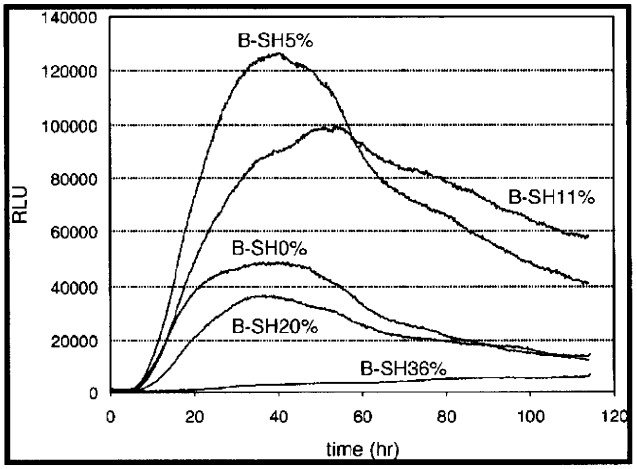

Figure 1. Real-time luciferase gene expression of the polyplex micelles with varying thiolation degrees at N/P = 2 against 293T cells.

Antitumor Activity. Polyplex micelles containing sFlt-1 pDNA were injected iv into mice bearing pancreatic adenocarcinoma BxPC3, followed by evaluation of tumor volume (Figure 2). All the micelles were injected three times on days

(17) Takae, S.; Miyata, K.; Oba, M.; Ishii, T.; Nishiyama, N.; Itaka, K.; Yamasaki, Y.; Koyama, H.; Kataoka, K. PEG-detachable Polyplex Micelles Based on Disulfide-crosslinked Block Cationers as Bioresponsive Nonviral Gene Vectors. *J. Am. Chem. Soc.* **2008**, *130*, 6001–6009.

(18) Oba, M.; Aoyagi, K.; Miyata, K.; Matsumoto, Y.; Itaka, K.; Nishiyama, N.; Yamasaki, Y.; Koyama, H.; Kataoka, K. Polyplex Micelles with Cyclic RGD Peptide Ligands and Disulfide Cross-links Directing to the Enhanced Transfection via Controlled Intracellular Trafficking. *Mol. Pharmaceutics* **2008**, *5*, 1080–1092.

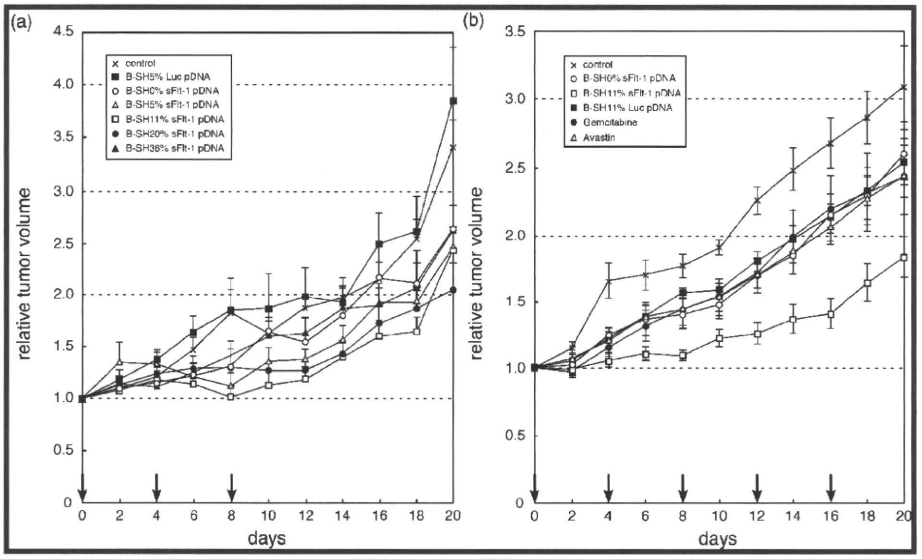

Figure 2. Antitumor activity of polyplex micelles with sFlt-1 pDNA in subcutaneously BxPC3-inoculated mice. (a) Effect of thiolation degree. Hepes buffer (control) was used as a negative control. Polyplex micelles were injected iv on days 0, 4, and 8 at 20 μg pDNA/mouse, and mice were monitored for the relative tumor volume every second day. Error bars represent the SEM ($n = 6$). Only the B-SH11% polyplex micelles exhibited significant retardation of tumor growth compared to the control ($P < 0.01$). (b) Growth curve study with an increased dose of the B-SH11% polyplex micelles compared to commercially available drugs. Polyplex micelles (20 μg pDNA/mouse), gemcitabine (100 mg/kg), and Avastin (50 mg/kg) were injected iv on days 0, 4, 8, 12, and 16. Relative tumor size was measured every second day. Hepes buffer (control) was used as a negative control. Error bars represent the SEM ($n = 5$). Only the B-SH11% polyplex micelles exhibited significant retardation of tumor growth compared to the control ($P < 0.001$). P values were calculated by multivariate ANOVA study.

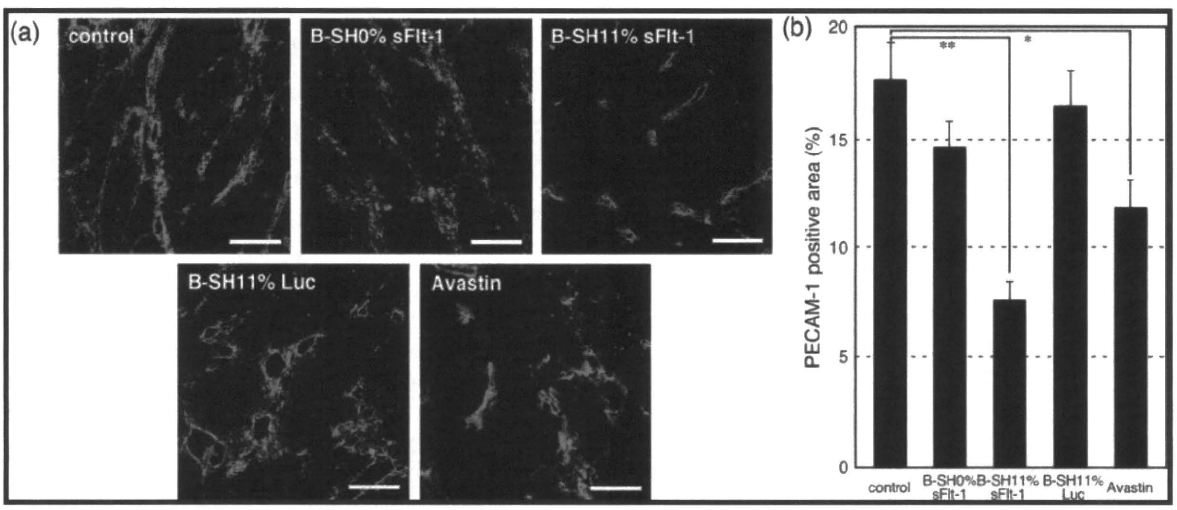

Figure 3. Immunostaining of the VECs in the BxPC3 tumor tissue by PECAM-1 antibody. Hepes buffer (control), three types of polyplex micelles (20 μg of pDNA/mouse), and Avastin (50 mg/kg) were injected into the BxPC3-inoculated mice via the tail vein on days 0 and 4. Mice were sacrificed on day 6, and tumors were excised and immunostained. (a) CLSM images of immunostained tumors. PECAM-1-positive regions are green. Bars represent 100 μm. (b) Areas of PECM-1-positive endothelium were quantified. Error bars represent the SEM ($n = 15$). P values were calculated by Student's t test. $^*P < 0.01$ and $^{**}P < 0.001$.

0, 4, and 8 (Figure 2a). The B-SH11% micelle significantly suppressed tumor growth compared to control mice treated with Hepes buffer ($P < 0.01$). There was no significant change in tumor growth after injection of other polyplex micelles, implying that an optimal cross-linking rate is required to achieve an effective expression of the gene. Encouraged by these results, the tumor growth suppression activity of B-SH11% micelle was further evaluated, implying a regimen with enhanced number of injections. The effect of the micelles was compared to commercially available drugs, gemcitabine, a standard chemotherapeutic agent for pancreatic tumor, and bevacizumab (Avastin), a monoclonal antibody against VEGF (Figure 2b). The doses of gemcitabine and Avastin implied in our study were based on

previous reports published elsewhere.[15,16] The administration of B-SH11%/sFlt-1 micelle resulted in significant suppression of tumor growth ($P < 0.001$), while gemcitabine and Avastin, under the reported experimental regimen, showed no remarkable therapeutic effect. Note that the difference observed in tumor volumes between the B-SH11%/Luc micelle-treated group and the control group was not significant.

Tumor Vascular Density. The antiangiogenic effect of expressed sFlt-1 was confirmed by immunostaining of VECs using PECAM-1 (Figure 3). Vascular density of tumors treated with either B-SH11%/sFlt-1 micelle or Avastin was significantly lower than that of the other groups. The most pronounced and significant effect on neo-vasculature suppression was achieved by B-SH11%/sFlt-1 micelle (7% PECAM-1 positive area) over Avastin (12% PECAM-1 positive area) ($P < 0.05$). These results suggest that the expressed sFlt-1 may entrap VEGF secreted in the tumor tissue, thereby suppressing the growth of VECs.

***In Vivo* sFlt-1 Gene Expression.** Expression levels of sFlt-1 in the body were then evaluated by measuring the amount of sFlt-1 in lung, liver, spleen, kidney, tumor, and blood plasma using enzyme-linked immunosorbent assay (ELISA) (Figure 4). Injection of B-SH11%/sFlt-1 micelle resulted in significantly higher expression of sFlt-1 selectively in tumor tissue compared to the control. On the other hand, injection of B-SH0%/sFlt-1 micelle or B-SH11%/Luc micelle did not result in any difference in sFlt-1 expression compared to the control. These results strongly support that tumor-specific elevation in sFlt-1 expression led to the significant growth suppression of VECs in the tumor tissue and, eventually, the suppression of tumor growth.

***In Vivo* Enhanced Green Fluorescence Protein (EGFP) Gene Expression in Tumors.** The location of gene expression in BxPC3 tumors after administration of the micelles was analyzed histologically using pDNA encoding EGFP (Figure 5). As previously reported,[13,19,20] thick fibrotic tissue was formed around blood vessels (red) inside the stroma of BxPC3 tumors, and nests of tumor cells (region T) were scattered in the stroma (Figure 5a). The expression of EGFP (Figures 5b and 5c) was observed mainly in the VECs and cells in stromal regions adjacent to some vasculature, indicating that VECs and fibroblasts near some vasculature in the stroma, but not the tumor cells, were transfected. As seen in Figure 5a, there were thick fibrotic tissues around blood vessels in the BxPC3 xenograft,

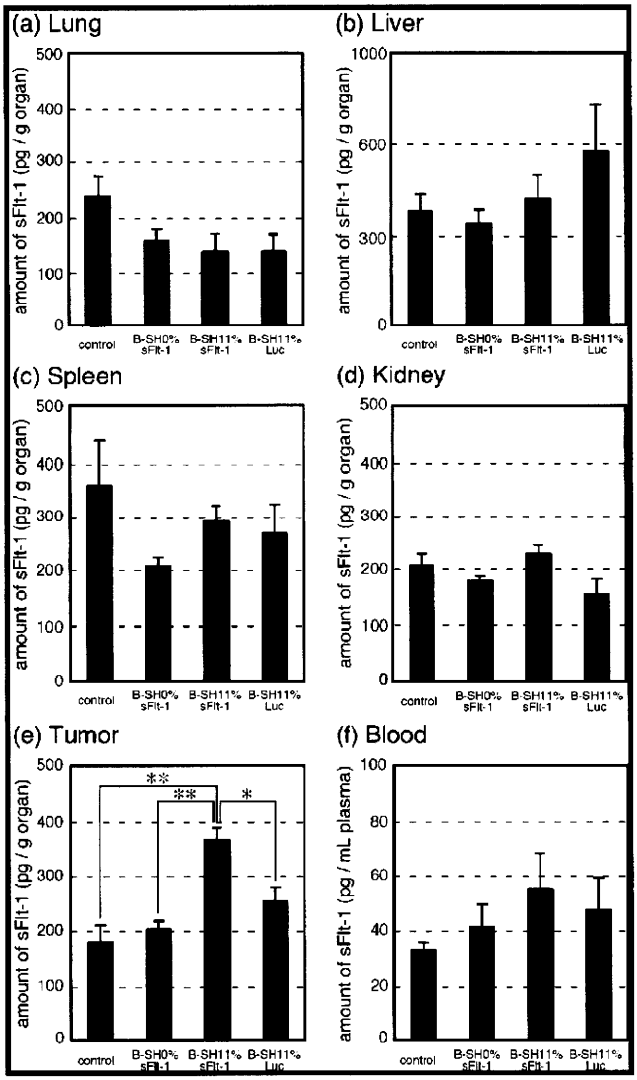

Figure 4. Evaluation of sFlt-1 gene expression in organs by ELISA. Hepes buffer (control) and three types of polyplex micelles (20 μg pDNA/mouse) were injected into the BxPC3-inoculated mice via the tail vein on days 0 and 4. Mice were sacrificed on day 6 after collecting blood (f), and the lungs (a), livers (b), spleens (c), kidneys (d), and tumors (e) were excised, followed by evaluation of sFlt-1 concentration by ELISA according to the manufacturer's protocol. Error bars represent the SEM ($n = 6$). P values were calculated by Student's t test. $^*P < 0.01$ and $^{**}P < 0.001$.

indicating that the penetration of polyplex micelles deep into the stroma or into the tumor nest was interrupted and the gene expression was limited in the VECs and some of the fibroblasts in the stroma. Higher levels of EGFP expression were observed for B-SH11% micelle, confirming their enhanced ability to accumulate inside tumor tissue compared to B-SH0% micelle.

Discussion

Since all solid tumors need angiogenesis for their growth, antiangiogenic therapy is a promising strategy for treating

(19) Miyata, K.; Oba, M.; Kano, M. R.; Fukushima, S.; Vachutinsky, Y.; Han, M.; Koyama, H.; Miyazono, K.; Nishiyama, N.; Kataoka, K. Polyplex Micelles from Triblock Copolymers Composed of Tandemly Aligned Segments with Biocompatible, Endosomal Escaping, and DNA-condensing Functions for Systemic Gene Delivery to Pancreatic Tumor Tissue. *Pharm. Res.* **2008**, *25*, 2924–2936.

(20) Kano, M. R.; Komuta, Y.; Iwata, K.; Oka, M.; Shirai, Y.; Morishita, Y.; Ouchi, Y.; Kataoka, K.; Miyazono, K. Comparison of the Effects of the Kinase Inhibitors Imatinib, Sorafenib, and Transforming Growth Factor-β Receptor Inhibitor on Extravasation of Nanoparticles from Neovasculature. *Cancer Sci.* **2009**, *100*, 173–180.

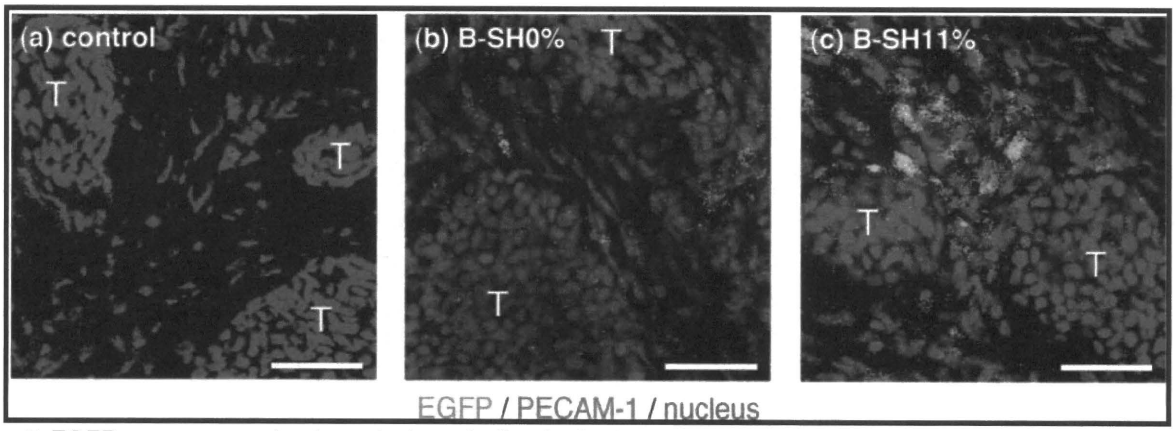

Figure 5. EGFP gene expression by polyplex micelles in the inoculated BxPC3 tumors. Hepes buffer (a) was used as a negative control. B-SH0% (b) and B-SH11% (c) polyplex micelles containing EGFP pDNA (20 μg pDNA/mouse) were injected into the BxPC3-inoculated mice via the tail vein. Mice were sacrificed on day 3, and tumors were excised and immunostained. "T" indicates nests of tumor cells in tumor tissues. Bars represent 50 μm.

tumor patients. In fact, Avastin, the recombinant humanized monoclonal antibody against VEGF, has been widely used as an antiangiogenic drug, and its application range is spreading to the various types of solid tumors.[16] Other antiangiogenic proteins,[21,22] e.g., angiostatin, endostatin, and soluble forms of VEGF receptor, have also received great attention. Meanwhile, antiangiogenic gene therapy represents an attractive alternative to antiangiogenic proteins for reasons such as low dose, continuous expression of the therapeutic protein, and low cost. Therefore, development of an effective and safe gene vector is a key to successful antiangiogenic gene therapy.

In this study, thiolated PEG-PLys block copolymers were applied in the formation of disulfide cross-linked polyplex micelles for delivery of pDNA encoding sFlt-1, and tested for their antiangiogenic effect on mice bearing xenografted BxPC3 cell line, derived from human pancreatic adenocarcinoma. Disulfide cross-links in the polyplex core were designed to increase blood stability of the polyplex micelles and effectively release pDNA in the intracellular milieu.[10,11,18] PEG palisade of the polyplex micelle is expected to cover the polyplex core to shield the positive charge as well as to decrease interfacial free energy.[12,23] The formation of the PEG palisade surrounding the polyplex core was confirmed by the neutral zeta-potential of the polyplex micelles (Table 1). B-SH36% micelle showed an approximately 10 times higher concentration of pDNA in the blood at 60 min after iv injection than that of the micelle without core cross-linking (B-SH0%) (Figure 4 in the Supporting Information). The disulfide cross-links in the polyplex core apparently contribute to the enhanced stability of the micelles in the bloodstream. Note that the size of polyplex micelles is between 100 and 150 nm (Table 1), which may be in a suitable range for accumulation in solid tumors due to the enhanced permeability and retention (EPR) effect,[24] although the size may be too large to allow the micelles to penetrate into the stroma in pancreatic tumors.[13] Nevertheless, there is a concern that excessive disulfide cross-links interfere with the smooth release of entrapped pDNA in the core, resulting in decreased transfection efficiency.[10] Accordingly, optimal cross-linking density should be determined to balance the stability and maintain high transfection efficiency. The results of *in vitro* real-time gene expression showed that B-SH5% micelle possessed the highest efficiency among the evaluated samples up to 60 h after transfection. It is noteworthy that B-SH11% micelle exerted sustained Luc expression and kept an appreciably high efficiency beyond 60 h (Figure 1). Apparently, gene expression is prolonged with an increase in cross-linking rates, although excess cross-links induced overstabilization of polyplex micelles, resulting in decreased transfection efficiency in the case of the B-SH20% and B-SH36% micelles. Eventually, the B-SH36%/sFlt-1 micelle had no *in vivo* efficiency, even though they showed the highest stability in the bloodstream among the evaluated samples (Figure 4 in the Supporting Information). It is also noteworthy that the B-SH11%/sFlt-1 micelle achieved an appreciably high therapeutic efficiency, even though it showed only limited improvement in blood circulation time compared to the B-SH0% and B-SH5% systems. Presumably, a sustained

(21) Sim, B. K. L.; MacDonald, N. J.; Gubish, E. R. Angiostatin and Endostatin: Endogenous Inhibitors of Tumor Growth. *Cancer Metastasis Rev.* **2000**, *19*, 181–190.

(22) Fischer, C.; Mazzone, M.; Jonckx, B.; Carmeliet, P. FLT1 and Its Ligands VEGFB and PlGF: Drug Targets for Anti-angiogenic Therapy. *Nat. Rev. Cancer* **2008**, *8*, 942–956.

(23) Kakizawa, Y.; Kataoka, K. Block Copolymer Micelles for Delivery of Gene and Related Compounds. *Adv. Drug Delivery Rev.* **2002**, *54*, 203–222.

(24) Matsumura, Y.; Maeda, H. A New Concept for Macromolecular Therapeutics in Cancer Chemotherapy: Mechanism of Tumoritropic Accumulation of Proteins and the Antitumor Agent Smancs. *Cancer Res.* **1986**, *46*, 6387–6392.

profile in gene expression may have been the key to this achievement. Note that no change in body weight of the mice was observed during the experiment (data not shown), indicating few serious side effects of polyplex micelles.

Comparison with the commercially available agents, gemcitabine and Avastin, confirmed the encouraging tumor growth suppression effect of the B-SH11% polyplex micelle (Figure 2b). Gemcitabine continues to be the standard therapy in the treatment of pancreatic tumors; however, its objective response rate is limited in patients with advanced disease.[25] Avastin is a recombinant humanized monoclonal antibody against human VEGF, which may neutralize tumor-cell-derived VEGF in the model used here. In humans, Avastin is the first clinically available antiangiogenic drug, and it has been efficient when used in combined chemotherapy for metastatic colorectal cancer[26] and non-small-cell lung cancer.[27] However, it showed no benefit in patients with pancreatic tumors.[25] The B-SH11%/sFlt-1 micelle significantly suppressed tumor growth compared not only to the control ($P < 0.001$) but also to the B-SH11%/Luc micelle, gemcitabine, and Avastin ($P < 0.01$) (Figure 2b). Xenografted BxPC3 was reported not to respond to gemcitabine,[28] probably due to its inability to penetrate through the tumor thick fibrotic tissue and target tumor cells, which is consistent with our results. Evaluation of vascular density in BxPC3 tumor (Figure 3) clearly showed that the B-SH11%/sFlt-1 micelle decreased vascular density compared to the control ($P < 0.001$), the B-SH11%/Luc micelle ($P < 0.001$), and Avastin ($P < 0.05$) treated tumors.

Inhibitory effect on tumor growth (Figure 2) is consistent with the result of decreased vascular density. There are several studies on antiangiogenic gene therapy for subcutaneously inoculated tumors in mice by systemic expression of sFlt-1 using viral vectors, including im injection of adeno-associated viral vectors[29] and iv injection of adenoviral vectors to target livers.[30] In these studies, however, sFlt-1 was expressed mainly in organs rather than tumor tissue. What was worse, the excess expression of sFlt-1 in the liver led to unacceptable hepatotoxicity.[31] Thus, tumor-specific expression of sFlt-1 is essential for a safe and efficient antiangiogenic gene therapy. However, any nonviral gene vectors loading sFlt-1 gene have failed to exhibit selective gene expression in the tumor tissue, although they achieved certain inhibition of tumor growth.[8,9] In this regard, the B-SH11%/sFlt-1 micelle system might be promising, since sFlt-1 expression was significantly increased selectively in the tumor tissue compared not only to the control ($P < 0.001$) but also to the B-SH11%/Luc micelle ($P < 0.01$), as shown in Figure 4, without any significantly enhanced expression in other normal tissues. Note that no significant increase of sFlt-1 expression was observed in any normal organs treated with B-SH0%/sFlt-1 micelle or B-SH11%/Luc micelle. Histological analyses revealed that EGFP expression of the B-SH11%/EGFP micelle was located mainly around VECs but not in the tumor cells (Figure 5), probably due to restricted permeation of micelles by thick fibrotic tissues and pericyte-covered vasculature of the BxPC3 tumors. These results suggested the ability of expressed sFlt-1 molecule to entrap excess VEGF in the tumor tissue and to inhibit tumor growth by an antiangiogenic effect. Xenografted BxPC3 tumors in mice are characterized by stroma-rich histology,[20] which might explain the only slight inhibitory effects on BxPC3 growth achieved by gemecitabine[28] targeting tumor cells.

Conclusions

In conclusion, antiangiogenic gene therapeutic study was carried out by iv administration of polyplex micelles with sFlt-1 pDNA to mice bearing pancreatic adenocarcinoma BxPC3 xenografts, and the results demonstrated the ability of B-SH11% sFlt-1 micelle as a safe and effective gene delivery system. The optimal disulfide cross-linking rate of polyplex micelles was found to show significant suppression of tumor growth. Gene expression of sFlt-1 by iv injection of polyplex micelles was observed in tumor tissue only, followed by decreased vascular density and significant suppression of tumor growth. Based on these results, the B-SH11% disulfide cross-linked polyplex

(25) Rocha-Lima, C. M. New Directions in the Management of Advanced Pancreatic Cancer: a Review. *Anti-Cancer Drugs* **2008**, *19*, 435–446.

(26) Hurwitz, H.; Fehrenbacher, L.; Novotny, W.; Cartwright, T.; Hainsworth, J.; Heim, W.; Berlin, J.; Baron, A.; Griffing, S.; Holmgren, E.; Ferrara, N.; Fyfe, G.; Rogers, B.; Ross, R.; Kabbinavar, F. Bevacizumab Plus Irinotecan, Fluorouracil, and Leucovorin for Metastatic Colorectal Cancer. *N. Engl. J. Med.* **2004**, *350*, 2335–2342.

(27) Sandler, A.; Gray, R.; Perry, M. C.; Brahmer, J.; Schiller, J. H.; Dowlati, A.; Lilenbaum, R.; Johnson, D. H. Paclitaxel-carboplatin Alone or with Bevacizumab for Non-small-cell Lung Cancer. *N. Engl. J. Med.* **2006**, *355*, 2542–2550.

(28) Merriman, R. L.; Hertel, L. W.; Schultz, R. M.; Houghton, P. J.; Houghton, J. A.; Rutherford, P. G.; Tanzer, L. R.; Boder, G. B.; Grindey, G. B. Comparison of the Antitumor Activity of Gemcitabine and Ara-C in a Panel of Human Breast, Colon, Lung and Pancreatic Xenograft Models. *Invest. New Drugs* **1996**, *14*, 243–247.

(29) Takei, Y.; Mizukami, H.; Saga, Y.; Yoshimura, I.; Hasumi, Y.; Takayama, T.; Kohno, T.; Matsushita, T.; Okada, T.; Kume, A.; Suzuki, M.; Ozawa, K. Suppression of Ovarian Cancer by Muscle-Mediated Expression of Soluble VEGFR-1/Flt-1 Using Adeno-associated Virus Serotype 1-derived Vector. *Int. J. Cancer* **2006**, *120*, 278–284.

(30) Liu, J.; Li, J.; Su, C.; Huang, B.; Luo, S. Soluble Fms-like Tyrosine Kinase-1 Expression Inhibits the Growth of Multiple Myeloma in Nude Mice. *Acta Biochim. Biophys. Sin.* **2007**, *39*, 499–506.

(31) Mahasreshti, P. J.; Kataram, M.; Wang, M. H.; Stockard, C. R.; Grizzle, W. E.; Carey, D.; Siegal, G. P.; Haisma, H. J.; Alvarez, R. D.; Curiel, D. T. Intravenous Delivery of Adenovirus-mediated Soluble FLT-1 Results in Liver Toxicity. *Clin. Cancer Res.* **2003**, *9*, 2701–2710.

micelle with sFlt-1 pDNA is interesting and worthy to develop further for antiangiogenic gene therapy of solid tumors.

Acknowledgment. This work was financially supported in part by the Core Research Program for Evolutional Science and Technology (CREST) from Japan Science and Technology Agency (JST) as well as by Grants-in-Aid for Young Scientists (A) and Exploratory Research. We express our appreciation to Masabumi Shibuya (Tokyo Medical and Dental University) for providing pVL 1393 baculovirus vector pDNA encoding human sFlt-1. We thank Kazuhiro Aoyagi, Yoko Hasegawa, Kotoe Date, and Satomi Ogura (The University of Tokyo) for technical assistance.

Supporting Information Available: Synthesis of thiolated block copolymer and Supporting Figures 1, 2, 3, and 4. This material is available free of charge via the Internet at http://pubs.acs.org.

MP9002317